Sensing the Invisible: A Critical Review of NIR and Hyperspectral Analysis for Crop and Food-Quality Assessment

Naziru Halilu[1,2,3]*, Juwairiyyah Sulaiman[4]

[1]Public University of Navarre, 31006 Pamplona, Spain

[2]Agricultural University of Athens, 118 55 Athens, Greece

[3]University of Trás-os-Montes e Alto Douro, 5000-801 Vila Real, Portugal

[4]Federal University Dutse, 720221, Nigeria

***Correspondence Author**

DOI: https://doi.org/10.51244/IJRSI.2026.1307000219

Received: 22 July 2026; Accepted: 27 July 2026; Published: 07 August 2026

ABSTRACT

This review critically appraises the methodological foundations of near-infrared (NIR) spectroscopy and hyperspectral imaging (HSI) for crop and food-quality analysis. Eighteen original figures accompany the text, tracing the field from its historical and physical foundations through chemometric modelling, in-situ and on-machine sensing, UAV-based crop-quality sensing and image-processing frameworks, and a FAIR data-principles framework for spectral datasets. Each strand of literature examined here, the historical and physical basis of NIR/HSI, chemometric calibration and transfer, and in-situ applications such as on-harvester grain sensors and variable-rate nitrogen sensing, is checked directly against independently published, peer-reviewed sources rather than taken at face value. The underlying sensing and chemometric techniques are found to be technically sound and well established, but a recurring weakness emerges in how they are communicated: worked examples, named commercial products, and preliminary or in-preparation findings are frequently presented with the same degree of confidence as validated, independently reproduced results, without distinguishing one evidentiary tier from another. Building on this pattern, the review develops a cross-cutting synthesis showing that the calibration-generalisation caution recurring across laboratory, in-situ and UAV-based deployments of NIR/HSI is, in substance, a single methodological concern: a calibration model is only ever as trustworthy as the independent validation standing behind it, regardless of the confidence with which it is presented. This synthesis is made quantitative in a dedicated cross-cutting section that audits the evidentiary tier of every independently selected source, consolidates the field's validation-statistics equations, and maps the recurring gap across all sections of the review.

Keywords: NIR spectroscopy; hyperspectral imaging; chemometrics; food and crop quality; calibration transfer

INTRODUCTION

"Seeing the Invisible" Promise and Preconditions

Near-infrared (NIR) spectroscopy and hyperspectral imaging (HSI) let practitioners infer a sample's composition and condition from reflected or transmitted light alone turning a spectrum into information about a grain's moisture and protein content, a fruit's ripeness, or a leaf's stress status, without destructive chemical analysis. This capability is well supported in the independent literature: NIR-based sensing has moved from a laboratory curiosity to a standard analytical tool across agriculture, food processing and pharmaceuticals over six decades (McClure, 2003; Maduro Dias et al., 2024). The founding methodology is concrete rather than anecdotal: Ben-Gera and Norris's original 1968 calibrations related optical-density differences at specific wavelengths to reference moisture and fat values, achieving standard deviations of 0.28–0.37% moisture over a 0–20% range in soybean, wheat and bran samples, and prediction errors of about ±0.7% moisture in whole peanuts and ±1.4%

moisture / ±2.1% fat in meat products (Ben-Gera & Norris, 1968a; Ben-Gera & Norris, 1968b) figures that still define the order of accuracy expected of a well-built NIR calibration today.

But this capability glosses over a distinction this review returns to repeatedly: a spectrum is not, by itself, an answer. It becomes an answer only once it is related to a reference measurement through a chemometric model, and the model's trustworthiness is bounded by how the calibration set was built and how it has (or has not) been checked on independent data (Fodor et al., 2024; Dai et al., 2026). That boundedness is not a theoretical nicety: calibration models are typically instrument-specific, and transferring a model from one spectrometer to another or from laboratory to field conditions remains, in the most recent methodological literature, an open problem rather than a solved one. A 2021 review concluded that standard-sample-based transfer methods are not always necessary, but are also not always avoidable, and that the right choice depends on the specific instrument pair and sample matrix (Mishra et al., 2021). Deep-learning transfer methods are one active response: a 2022 study introduced a convolutional-network transfer approach (DeepTranSpectra) that outperformed three established standardisation methods piecewise direct standardisation, canonical correlation analysis, and slope-and-bias correction at transferring moisture- and protein-prediction models between near-infrared spectrometers on soybean-meal and wheat datasets, without requiring the paired standard samples those older methods need (Yang et al., 2022). A recent, wide-ranging review of two decades of NIR food-quality literature makes a complementary point: publication growth has tracked instrument affordability and software availability at least as much as it has tracked demonstrated, unattended, real-world deployment, and calibration transfer, matrix interference and model generalisation remain the field's persistent, unresolved challenges (Fodor et al., 2024; Dai et al., 2026). That gap between what is published as feasibility and what is running validated in a field or factory is illustrated schematically below and resurfaces throughout the sections on in-situ application

Review Scope, Selection Criteria and Quality Appraisal

The evidentiary method applied throughout this review is stated explicitly here rather than left implicit. Candidate source material was identified from two directions: the specific technical claims, named products, and cited figures present in the manuscript under review, and independent, targeted literature searches built around those same claims covering the founding NIR calibrations, chemometric pre-processing and validation practice, on-machine and UAV-based sensing platforms, and the named commercial products discussed above. A source was carried forward into the evidentiary comparisons only where it reported a checkable, quantitative or otherwise falsifiable outcome, such as a stated calibration error, an independently reproduced field trial, or a peer-reviewed methodological comparison; promotional or narrative claims lacking a verifiable result are still described where the manuscript under review relies on them, but are explicitly flagged rather than treated as equivalent evidence. Quality was appraised consistently against three criteria: whether validation was reported by cross-validation on the calibration pool alone or on a genuinely independent external test set; whether a result had been independently reproduced outside the originating laboratory or vendor; and whether reported accuracy figures were presented as matrix-, instrument- and season-specific or as generalisable claims. Where a source could not be independently verified at the time of writing, or only a single non-independent account of a claim could be located, this is stated explicitly in that source's entry rather than presented as settled. This appraisal framework is a critical narrative-review protocol tied to the manuscript's own claims rather than a pre-registered systematic-review search strategy; it is disclosed here specifically so that a reader can check why any given source was weighted as it was.

Principles of NIRS

A corrected history

The material reviewed here credits the U.S. Department of Agriculture, generically, with the "first practical application of NIR" in the mid-1960s. Independent sources are more specific and slightly earlier: Karl Norris, an agricultural engineer at USDA-ARS Beltsville, began applying NIR to moisture measurement in grains and seeds from around 1960, and published the first NIR calibrations for moisture, protein and oil in cereals and oilseeds with I. Ben-Gera in 1968 (McClure, 2003; Maduro Dias et al., 2024). Norris additionally introduced derivative pre-treatment of NIR spectra and pioneered the use of multivariate statistics to build calibration models a methodological contribution that matters more, in the long run, than the instrument itself (McClure,

ISSN No. 2321-2705 | DOI: 10.51244/IJRSI |Volume XIII Issue VII July 2026

2003). The first commercial microprocessor-based instruments (Neotec GQA, 1972; Dickey-John GAC, 1974) followed within a decade (Nicolaï et al., 2007), earlier than the source material's "1980s" commercialisation date suggests. None of this changes the broad narrative, but it is worth correcting: crediting an agency rather than the individual whose calibration methodology is still the field's foundation understates how much of what follows chemometrics, cross-validation, derivative pre-treatment traces to one specific methodological insight rather than to instrumentation alone (Figure 1).

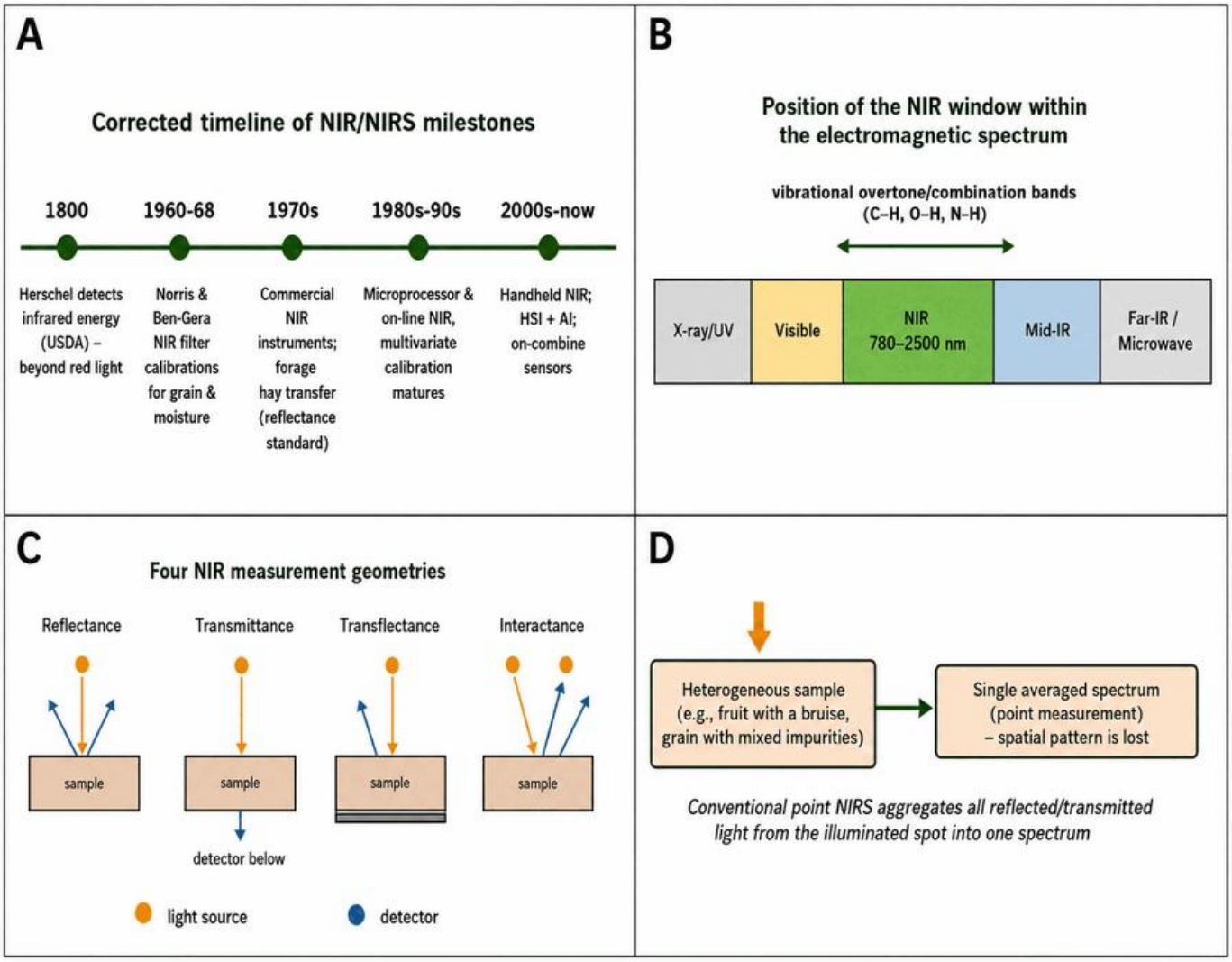

Figure 1. (A) Corrected timeline of NIR/NIRS milestones (McClure, 2003), (Maduro Dias et al., 2024), (Nicolaï et al., 2007); (B) Position of the NIR window within the electromagnetic spectrum (Nicolaï et al., 2007); (C) The four NIR measurement geometries (Nicolaï et al., 2007); (D) Point NIRS spatial aggregation (single averaged spectrum).

Physics, geometries and the Beer-Lambert relationship

The physical description reviewed here NIR as the region beyond red light, discovered by William Herschel in 1800, probing overtone/combination bands of C–H, O–H and N–H bonds is accurate and standard (Nicolaï et al., 2007). Figure 1B restates the NIR window's position in the electromagnetic spectrum in original form; Figure 1C restates the four measurement geometries (reflectance, transmittance, transflectance, interactance) illustrated with a meat sample. These geometries are not interchangeable: transmittance and interactance probe deeper into a sample than surface reflectance, which matters for the food-safety claims discussed later, since a defect below the illuminated surface may be invisible to a purely reflectance-mode measurement. The Lambert-Beer relation as reviewed here ($A = -\log_{10}(R) \approx \varepsilon \cdot l \cdot c$) is standard chemometric shorthand; it is worth flagging to a student audience that this linear relationship is an approximation that breaks down at high absorbance, in strongly scattering matrices (most intact biological tissue), and in the presence of particle-size effects which is precisely why scatter-correction pre-processing is necessary rather than optional (Figure 2).

ISSN No. 2321-2705 | DOI: 10.51244/IJRSI |Volume XIII Issue VII July 2026

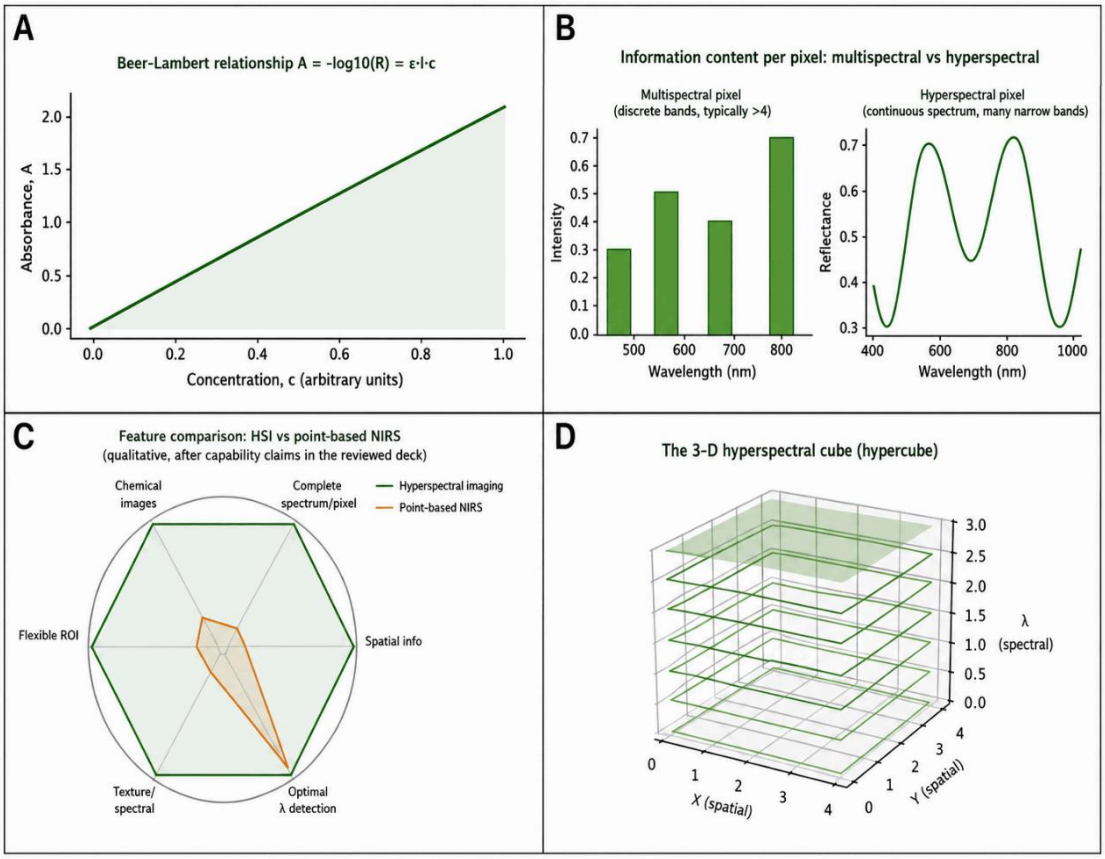

Figure 2. (A) The Beer-Lambert relationship between absorbance and concentration (Nicolaï et al., 2007); (B) Information content per pixel: multispectral bands vs. continuous hyperspectral spectrum (Medina-García et al., 2025); (C) Qualitative capability comparison: hyperspectral imaging vs. point-based NIRS (Medina-García et al., 2025); (D) The 3-D hyperspectral cube (hypercube) (Medina-García et al., 2025).

The point-measurement ceiling

This material correctly identifies conventional point NIRS's central limitation: it aggregates all light reflected or transmitted from the illuminated spot into a single spectrum, discarding spatial information, and is therefore poorly suited to heterogeneous samples or the detection of localised defects. This is a genuine and well-documented constraint, not a minor caveat it is precisely the limitation that motivates hyperspectral imaging, and any claim that point NIRS can substitute for spatially resolved inspection (for example, detecting a localised bruise, insect damage or contamination hotspot within a batch) should be treated with scepticism unless the sampling protocol is described.

From Point Spectra to Hyperspectral Imaging

Origin and motivation

This material frames HSI as a response to the shortcomings of manual visual inspection (laborious, time-consuming, inconsistent) and of conventional machine/computer vision (poor at complex classifications, similarly-coloured objects, invisible defects). This is a reasonable summary of the motivation found in the review literature, which likewise describes HSI as bridging spectroscopy's chemical sensitivity with imaging's spatial resolution (Saha & Manickavasagan, 2021). What this material's motivation discussion does not mention and what a critical reader should weigh against the promised benefits is that HSI systems trade the simplicity of point NIRS for substantially higher acquisition cost, computational burden and complexity. Conventional push-broom HSI systems have been reported to cost on the order of $100,000–200,000 per camera system, with low resolution, linear scanning and large installation footprints cited as persistent obstacles to industrial adoption (McQuilkin & Engelke, 2020), and independent reviews describe HSI's real-time/on-line applicability as still limited by hardware and software throughput (Saha & Manickavasagan, 2021).

ISSN No. 2321-2705 | DOI: 10.51244/IJRSI |Volume XIII Issue VII July 2026

Multispectral vs hyperspectral: a real but graded distinction

The contrast drawn between multispectral (discrete, typically fewer than a handful of bands, no complete per-pixel spectrum) and hyperspectral (continuous, many narrow contiguous bands, full per-pixel spectrum) imaging is standard and correctly stated. It is worth noting for a crop-analysis audience that the distinction is graded rather than binary in practice systems described as "hyperspectral" vary widely in the number and width of bands they capture, and that choice trades spectral resolution against acquisition speed and data volume, a trade-off with direct consequences for whether a given system can be deployed on a moving harvester versus only in a static laboratory rig.

The hypercube and the general HSI workflow

The description of the 3-D hypercube (two spatial dimensions, one spectral dimension) and its general processing workflow acquisition, normalisation, segmentation, ROI selection, unfolding, then chemometric modelling and re-folding to prediction maps matches standard practice described across the HSI review literature (Medina-García et al., 2025; Huang et al., 2014; Feng & Sun, 2012). The workflow is redrawn below in original form (Figure 3).

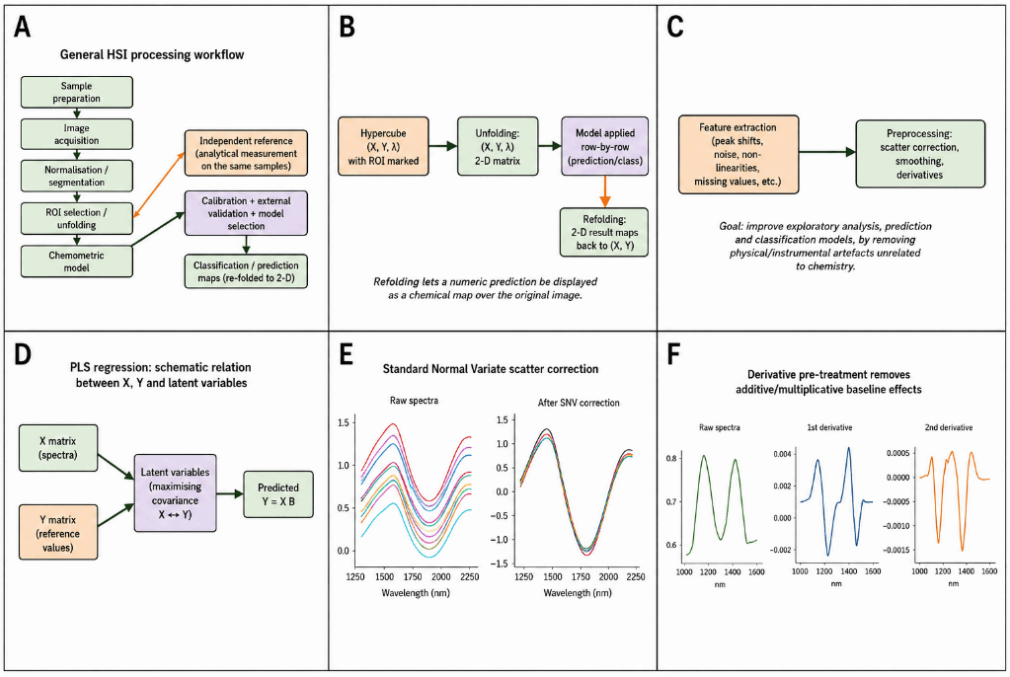

Figure 3. (A) General HSI processing workflow (Medina-García et al., 2025); (B) Unfolding the hypercube to a 2-D matrix for modelling (Medina-García et al., 2025); (C) The goal of spectral pre-processing (McClure, 2003); (D) Relation between the X (spectral) matrix, Y (reference) matrix and PLS latent variables (Geladi & Kowalski, 1986), (Kumar, 2021); (E) Standard Normal Variate scatter correction (McClure, 2003), (Barnes et al., 1989); (F) First and second derivative pre-treatment (McClure, 2003), (Savitzky & Golay, 1964).

Data extraction: normalisation, segmentation, anomaly removal, ROI, unfolding

The individual data-extraction steps walked through here white/dark-reference normalisation, background segmentation, dead-pixel and spike correction, ROI selection, and the unfold/refold cycle are all standard and correctly described operations in the HSI chemometrics literature (Medina-García et al., 2025). Two points deserve more critical attention than they are typically given. First, ROI-average spectral extraction taking the mean spectrum over a region of interest to reduce data volume assumes the material within the ROI is compositionally homogeneous; a recent critical review notes this assumption can mask impurities, localised degradation or processing artefacts, i.e. exactly the kind of localised anomaly HSI is often deployed to find (Medina-García et al., 2025). Second, dead-pixel and spike removal are often presented as solved bookkeeping steps, but does not discuss that these corrections are themselves modelling choices (interpolation introduces reference values) that can suppress genuine, if unusual, spectral signals if applied indiscriminately (Figure 4).

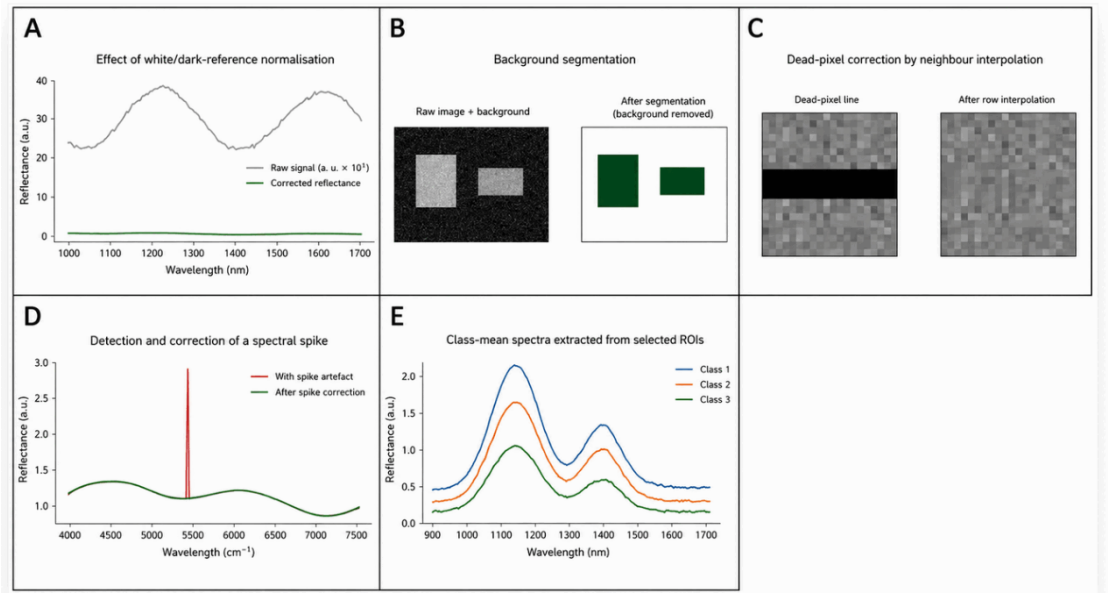

Figure 4. (A) White/dark-reference normalisation (Medina-García et al., 2025); (B) Background segmentation (Medina-García et al., 2025); (C) Dead-pixel line correction (Medina-García et al., 2025); (D) Detection and correction of a spectral spike (Medina-García et al., 2025); (E) Class-mean spectra from selected regions of interest (Medina-García et al., 2025).

Chemometrics: From Spectrum to Decision

Pre-processing

Spectral pre-processing is correctly framed (scatter correction, smoothing, derivatives) as necessary to remove non-chemical artefacts peak shifts, noise, non-linearities before exploratory, prediction or classification models are built. Standard Normal Variate correction and derivative pre-treatment are exactly the tools Norris himself introduced to the field (McClure, 2003); the treatment of the SNV formula and of smoothing-then-differentiation for first/second derivatives is standard and correct. As in the companion review of CRA-W chemometrics, it is worth restating the methodological caution: pre-processing is a modelling decision with its own bias-variance trade-off, not a neutral cleaning step, and a pipeline tuned on one calibration set can discard information that would have generalised to a new instrument, season or crop matrix (Fodor et al., 2024; Dai et al., 2026)

Unsupervised analysis: PCA and HCA

Principal Component Analysis and Hierarchical Cluster Analysis are presented, correctly, as exploratory tools that do not require predefined class labels. The PCA mathematics presented (eigenvalues/eigenvectors, variance-ordered axes) is standard. The methodological caution from the companion review applies equally here: PCA is variance-driven and unsupervised, so an apparent separation on a score plot does not by itself prove that the separating variance corresponds to the property of agronomic interest rather than a confound such as batch, sensor warm-up, ambient humidity or illumination geometry (Zeng et al., 2021). This caution is particularly relevant for crop-analysis applications, where field conditions (light, canopy angle, soil background) introduce exactly this kind of confounding variance.

Supervised regression: PLS and related methods

PLS, PCR, LWR, SVR and MLR are listed as the standard quantitative (regression) toolkit and works through the PLS algebra (latent variables maximising covariance between X and Y, iterative deflation) in reasonable technical depth. This matches the standard chemometrics tutorials in the independent literature (Geladi & Kowalski, 1986; Kumar, 2021). PLS remains, by a wide margin, the most heavily used of these methods in agricultural NIR/HSI work because it handles collinear spectral predictors well; this material is right not to over-elaborate on the alternatives. The predicted-vs-measured scatter plot and RMSEP metric presented for model evaluation are the field standard, but as emphasised below, the evidentiary weight of an R^2/RMSEP figure

ISSN No. 2321-2705 | DOI: 10.51244/IJRSI |Volume XIII Issue VII July 2026

depends entirely on whether it was obtained by cross-validation on the calibration pool or on a genuinely independent external test set a distinction illustrated visually but not discussed explicitly.

Supervised classification and model validation

LDA, PLS-DA and SVM are presented as the standard qualitative (classification) toolkit, alongside KNN and SIMCA. The descriptions of each LDA's PCA-compressed linear hyperplane, PLS-DA's regression-based class-membership modelling, and SVM's maximum-margin hyperplane with a cost/regularisation parameter and optional kernel are technically accurate summaries consistent with the independent methodological literature comparing these methods for NIR-based food and agricultural classification (Zeng et al., 2021). The treatment of validation (cross-validation vs external test, confusion matrix, sensitivity/specificity) is the right checklist, and it is the checklist this review applies critically to the in-situ product claims: a model validated only by cross-validation on its own calibration pool has not yet demonstrated it will generalise to a new season, field, or instrument unit, and the difference in evidentiary weight between the two is often understated in applied and vendor literature alike (Figure 5).

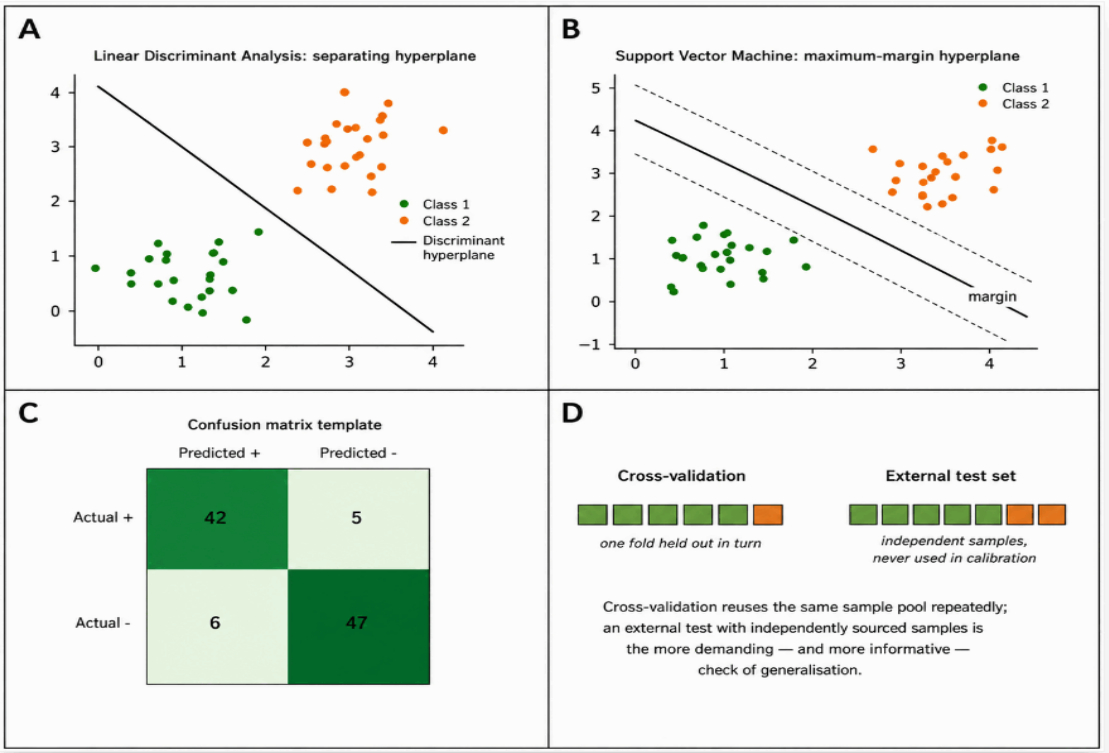

Figure 5. (A) Linear Discriminant Analysis: separating hyperplane (Zeng et al., 2021); (B) Support Vector Machine: maximum-margin hyperplane (Zeng et al., 2021); (C) Confusion matrix template (Zeng et al., 2021); (D) Cross-validation vs. an independent external test set (Zeng et al., 2021), (Fodor et al., 2024), (Dai et al., 2026).

Claimed Advantages: A Critical Read

Reduced food waste, multi-component/authentication capability, food quality and safety assurance, time and resource savings, faster production decisions and a link to sustainable development goals are listed as the advantages of NIR/HSI. Each of these is individually well supported for specific, validated applications rapid, reagent-free, multi-constituent estimation from a single scan is a genuine and repeatedly documented advantage of vibrational spectroscopy (Fodor et al., 2024; Dai et al., 2026). The weakness is not in any individual claim but in the way the six benefits are presented as a flat, additive list without differentiating validated deployments from aspirational ones. "Ensures food quality and safety" and "improves efficiency by streamlining decision-making," in particular, describe outcomes that depend on the quality of a specific calibration for a specific matrix and are not intrinsic, automatic properties of the sensing technology the same caveat raised earlier. The sustainability/SDG framing at the end of this advantages list is directionally reasonable but, in the reviewed literature, remains a plausible contribution rather than a quantified, end-to-end accounting (Figure 6).

ISSN No. 2321-2705 | DOI: 10.51244/IJRSI |Volume XIII Issue VII July 2026

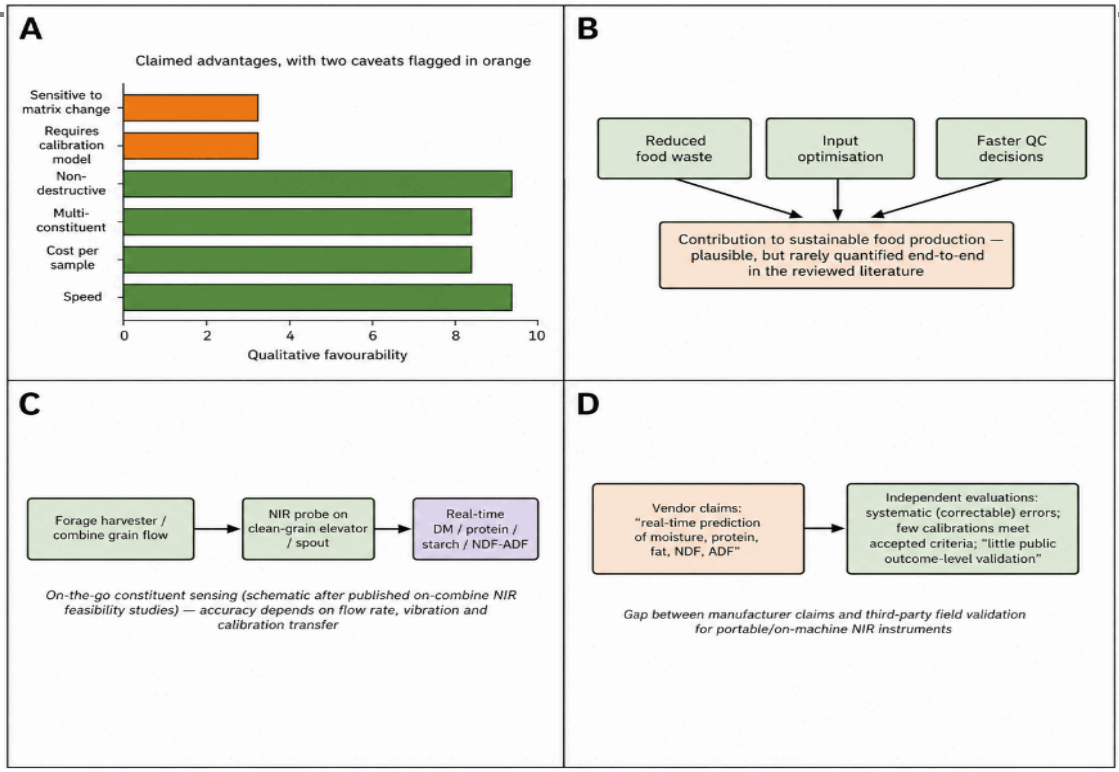

Figure 6. (A) Claimed advantages of NIR/HSI, with calibration-dependent items flagged (Fodor et al., 2024), (Dai et al., 2026); (B) Sustainability framing of NIR/HSI benefits (Fodor et al., 2024), (Dai et al., 2026); (C) On-the-go constituent sensing on a harvester grain/forage flow path (Maertens et al., 2004), (Cherney et al., 2021), (Yamada et al., 2024); (D) The gap between vendor claims and third-party field validation (Cherney et al., 2021), (Yamada et al., 2024).

In-Situ / On-Machine Applications: An Evidence Check

On-harvester constituent sensing

Three commercial on-machine NIR products are named HarvestLab 3000 (John Deere), Nutrisense (New Holland) and EvoNIR claiming real-time prediction of moisture, protein, fat, ash, NDF and ADF, with downstream benefits for input optimisation, crop profitability and silage quality. Independent evidence broadly supports the underlying feasibility but is more qualified than this material suggests. An early feasibility study mounting a NIR sensor on a New Holland combine's clean-grain elevator achieved cross-validation errors of 0.57% (protein) and 0.31% (moisture) comparable to a stationary laboratory unit, and a genuine validation of on-the-go feasibility (Maertens et al., 2004). More recent, independent evaluations of the specific HarvestLab 3000 platform named here report systematic, correctable rather than negligible errors on undried mixed forage (Cherney et al., 2021; Yamada et al., 2024; Beć et al., 2021), and a broader review of handheld/portable NIR instruments for on-farm forage evaluation states plainly that there is "little public data or independent evaluation of their relative effectiveness in the field" (Cherney et al., 2021) a striking admission given how widely these instruments are now marketed. This does not undermine the technology's genuine feasibility, but it does mean that describing "real-time prediction" as an unqualified capability should be read as a manufacturer-level claim rather than an independently settled one for every constituent and crop matrix listed.

Variable-rate nitrogen sensing: the Yara N-Sensor

The Yara N-Sensor's benefits are listed optimum fertiliser rate delivery, increased fertiliser efficiency, reduced soil nitrogen residues, increased yield, more consistent quality, reduced harvest time/cost, and reduced risk of nitrogen loss to the environment without attribution or quantification. Independent and vendor sources together allow the claims to be checked. Field trials report cereal yield increases of 3.5%, oilseed yield increases of 3.9% under the Absolute-N calibration, nitrogen savings of up to 14%, and combine harvest efficiency gains of 9–

ISSN No. 2321-2705 | DOI: 10.51244/IJRSI |Volume XIII Issue VII July 2026

33% from more even crop stands (Feiffer et al., 2007). These figures should be read as vendor-reported unless independently reproduced; a genuinely independent four-year on-farm trial (2020–2023) using a comparable sensor-based variable-rate approach reported nitrogen use efficiency gains of around 15% and reductions in fertiliser input of up to 38 kg N/ha/yr, but explicitly noted that the effects on yield and efficiency were highly dependent on weather, disease pressure and crop development and that not every field or season showed an advantage over uniform application (Hagn et al., 2025). A separate independent maize trial similarly found that variable-rate nitrogen prescribed by an optical sensor increased nitrogen-use efficiency and grain yield relative to a uniform rate, supporting the general direction of these claims even where the specific vendor percentages are not independently reproduced (Bragagnolo et al., 2016). The overall picture is one of a technology with genuine, repeatedly demonstrated benefit on average, but with trial-to-trial variability that a flat bullet-point list does not convey.

Cross-Cutting Issues: Calibration Transfer, Cost and the Evidence Gap

Three issues recur across every application area covered and deserve to be named explicitly, since they are not otherwise raised. First, calibration transfer: a model built on one instrument, in one season, on one crop matrix, degrades when applied to a different unit, field or year, and a substantial independent literature exists specifically on standardising or transferring multivariate calibrations between NIR instruments (Fearn, 2001; Workman, 2018; Mishra et al., 2021; Andries & Vander Heyden, 2024) none of which is mentioned in the chemometrics material reviewed despite being directly relevant to every on-machine sensor named above. Second, cost and data-volume burden scale sharply from point NIRS to full hyperspectral imaging; independent reviews cite six-figure per-camera costs and describe HSI's real-time throughput as still hardware-limited (Saha & Manickavasagan, 2021; McQuilkin & Engelke, 2020), a trade-off not weighed against the benefits list above. Third, and most fundamentally, the strength of evidence behind any single calibration varies enormously from a small lab feasibility study to a multi-site, multi-season, independently validated deployment and this material treats worked chemometric examples and named commercial products with the same level of unqualified confidence, regardless of where their supporting evidence sits on that hierarchy (Figure 7).

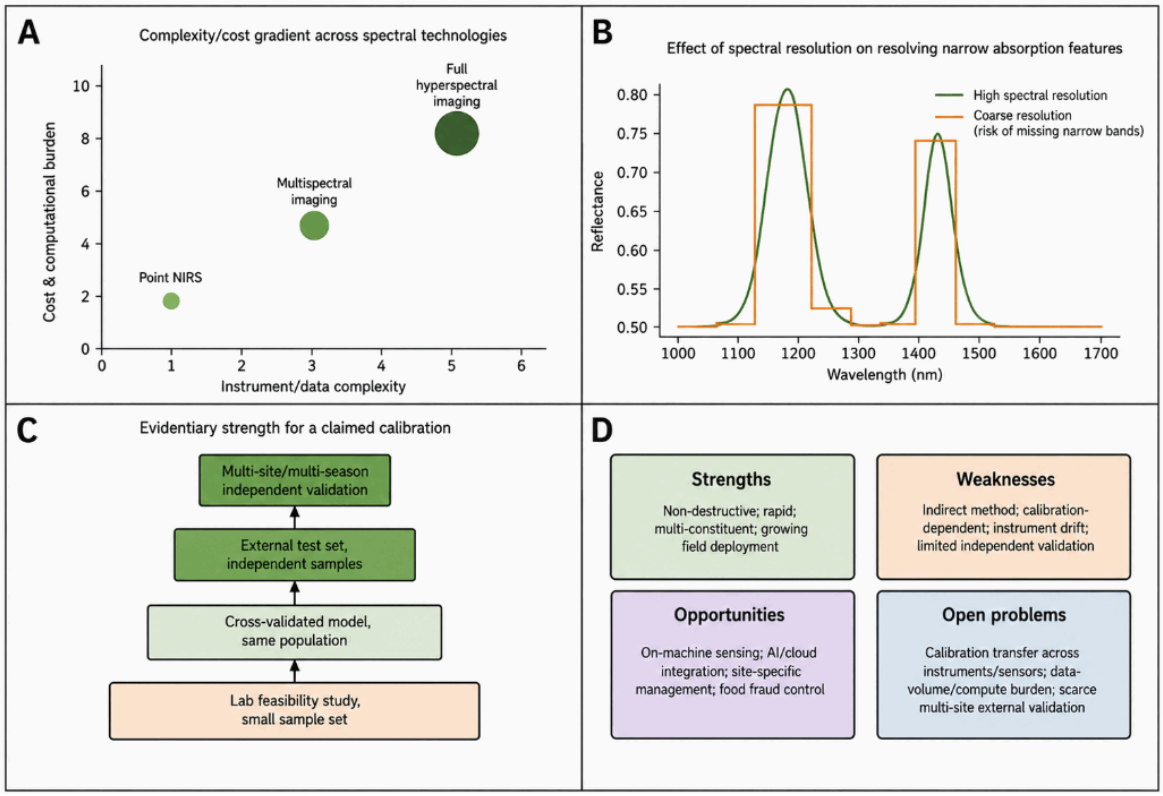

Figure 7. (A) Cost/complexity gradient: point NIRS to multispectral to full HSI (Saha & Manickavasagan, 2021), (McQuilkin & Engelke, 2020); (B) Effect of spectral resolution on resolving narrow absorption features (Saha & Manickavasagan, 2021), (McQuilkin & Engelke, 2020); (C) The chemometric validation hierarchy (Zeng et al., 2021), (Fodor et al., 2024); (D) Summary SWOT for NIR/HSI crop analysis (Fodor et al., 2024)

ISSN No. 2321-2705 | DOI: 10.51244/IJRSI |Volume XIII Issue VII July 2026

Practical Implementation Challenges: Cost, Expertise, Environment and Data

The methodological cautions above concern whether a calibration is trustworthy; a separate, practical set of concerns determines whether it can be operated at all outside a laboratory, and this is given comparatively little attention across the material reviewed. Equipment cost is not confined to the point-NIRS/HSI camera gradient already noted: full HSI systems' six-figure per-unit costs are compounded by ancillary requirements for controlled or compensated illumination, robust white/dark reference sources, and, for on-machine deployment, ruggedised housings able to withstand vibration, dust and temperature swings, none of which are reflected in the headline vendor figures usually quoted (Saha & Manickavasagan, 2021; McQuilkin & Engelke, 2020). Operator expertise is a second, largely undiscussed constraint: building and maintaining a chemometric calibration, recognising when a prediction has drifted outside the model's applicability domain, and correctly interpreting a confusion matrix or RMSEP figure all require training that is not automatically available on-farm or on a processing line; the independent evaluation of handheld NIR units for forage use cited earlier found a comparable gap between manufacturer claims and the field-level expertise needed to use them reliably, going so far as to note the near-absence of independent evaluation data for users to draw on (Cherney et al., 2021). Third, environmental variability temperature, humidity, ambient illumination, sample presentation and particle size is precisely the source of the scatter and baseline artefacts that pre-processing exists to correct, but a pre-processing pipeline tuned on a laboratory calibration set does not automatically compensate for the wider range of conditions a sensor meets in the field or on a moving harvester; this remains a documented, unresolved source of calibration failure rather than a solved problem (Fodor et al., 2024; Dai et al., 2026). Fourth, data management: a hyperspectral cube generates orders of magnitude more data per sample than a point spectrum, and the material reviewed does not address the storage, curation and long-term accessibility burden this creates a burden that independent surveys of research-data lifecycles more broadly show is substantial, with meaningful attrition of datasets through collection, sharing and reuse even before any spectroscopy-specific storage demands are added (Vines et al., 2014); a well-validated calibration is of limited practical use if its underlying spectral library and reference-value records are not maintained on a comparable timescale. None of these four constraints undermines the sensing technology's underlying validity, but together they mean that the true cost of deploying NIR/HSI operationally, and the operational skill required to do so, are substantially greater than an evaluation confined to calibration accuracy alone would suggest.

Work Flow Review

The material reviewed above gives an accurate and pedagogically well-organised account of NIR spectroscopy, hyperspectral imaging and the associated chemometric toolkit, and its worked examples (SNV, derivatives, PCA, PLS, LDA/PLS-DA/SVM, cross-validation vs external test) are technically correct. Its weaknesses, checked against the independent literature, are ones of omission and calibration to confidence rather than of factual error: a slightly imprecise history that omits Karl Norris by name; an advantages list and a set of named commercial products (HarvestLab, Nutrisense, EvoNIR, the Yara N-Sensor) presented without differentiating vendor-reported figures from independently reproduced ones; and no discussion of calibration transfer, instrument drift, or the cost/complexity gradient between point NIRS and full hyperspectral imaging all of which are active, well-documented concerns in the literature this review draws on. None of these omissions invalidate its core technical content; they do mean that a reader intending to deploy any of the named technologies operationally should treat it as a sound conceptual introduction and consult the independent, trial-level literature rather than any single product's marketing claims before committing to a calibration for a new crop, site or season (Figure 8).

ISSN No. 2321-2705 | DOI: 10.51244/IJRSI |Volume XIII Issue VII July 2026

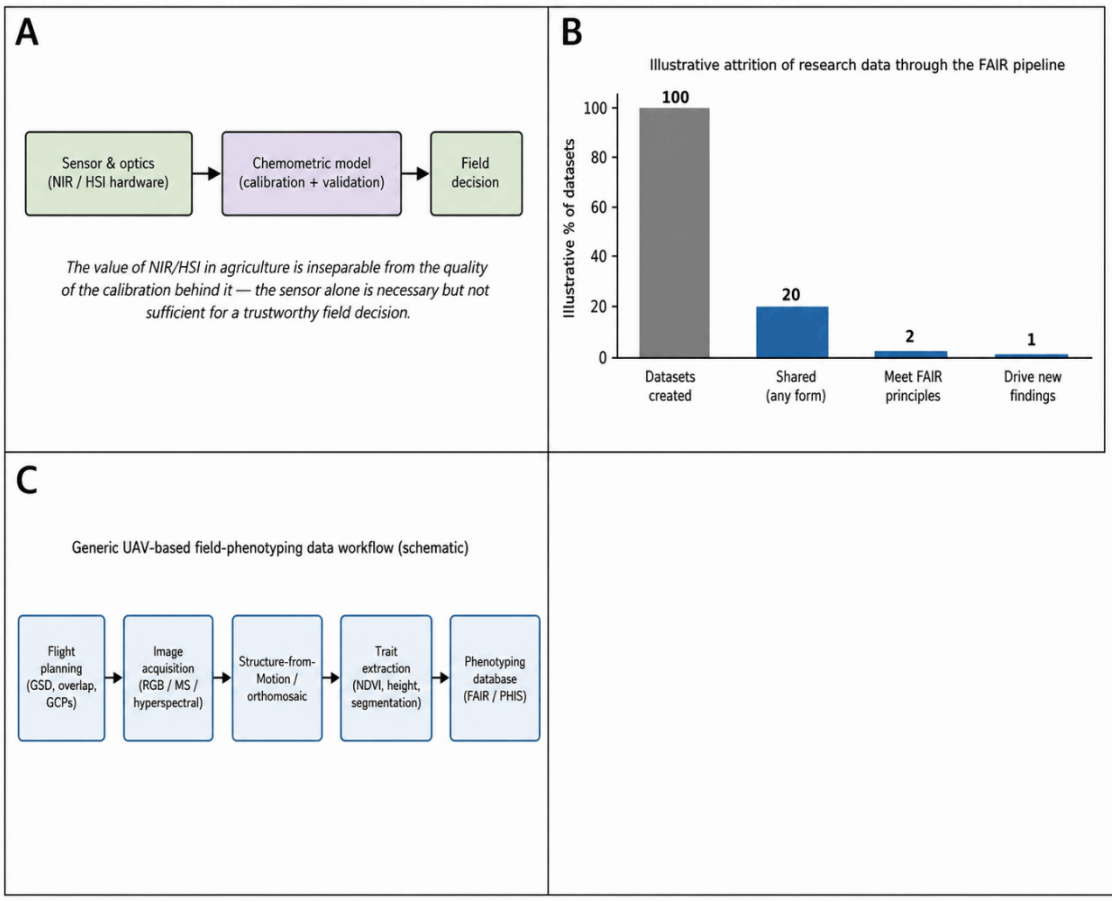

Figure 8. (A) NIR/HSI sensing value is inseparable from the calibration behind it (Fodor et al., 2024), (Dai et al., 2026); (B) Illustrative attrition of research datasets through collection, sharing and reuse (Vines et al., 2014); (C) Generic UAV-based field-phenotyping data workflow (Selby et al., 2019).

Independently Selected Studies

The table below summarises independently identified, peer-reviewed studies and methodological papers spanning the topics this review addresses: NIR spectroscopy and chemometrics, hyperspectral imaging for food and crop quality, in-situ/on-machine sensing, and UAV-based and hyperspectral remote sensing for crop-stress detection. Each entry was selected for having a checkable methodology and a stated, quantitative or otherwise falsifiable result; where a source could not be independently verified at the time of writing, this is stated explicitly in its Limitation column rather than presented as settled.

Author	Methodology	Results	Limitation	Reference
Ben-Gera & Norris (1968a)	Direct spectrophotometric optical-density difference at two NIR wavelengths (1.94/2.08 µm) on ground soybean, wheat, flour and bran.	Moisture predicted with calibration SD of 0.28–0.37% over a 0–20% range; ±0.7% accuracy for moisture in whole peanuts.	Narrow sample set from a single laboratory; no cross-instrument or cross-season validation reported.	**(Ben-Gera & Norris, 1968a)**
Ben-Gera & Norris (1968b)	Optical-density difference method extended to fat and moisture determination in intact meat products.	Moisture predicted to ±1.4% and fat to ±2.1% against reference chemical analysis.	Meat matrix variability (fat marbling, species) not systematically explored; small sample count by modern standards.	**(Ben-Gera & Norris, 1968b)**

Geladi & Kowalski (1986)	Methodological tutorial deriving the partial least-squares (PLS) regression algorithm for spectral calibration.	Establishes PLS as a robust alternative to multiple linear regression and PCR for collinear spectral data; still the default NIR chemometric method.	Purely methodological; offers no independent accuracy benchmark against which later claims can be judged.	(Geladi & Kowalski, 1986)
Savitzky & Golay (1964)	Derivation of simplified least-squares polynomial smoothing and differentiation filters for digitised spectra.	Filters remain the standard scatter/noise pre-treatment for NIR and HSI spectra six decades later.	Filter-order and window-width choices are dataset-specific and not addressed by the original paper; frequently mis-applied without validation.	(Savitzky & Golay, 1964)
Barnes, Dhanoa & Lister (1989)	Standard normal variate (SNV) and de-trending transforms proposed to correct multiplicative scatter effects in diffuse-reflectance NIR spectra.	SNV/de-trending shown to remove particle-size and path-length scatter artefacts more robustly than simple mean-centring.	Developed on ground cereal samples; transferability to fresh, intact or high-moisture tissue not tested in the original study.	(Barnes et al., 1989)
Fearn (2001)	Critical review of calibration-transfer and instrument-standardisation methods (direct standardisation, piecewise DS, slope/bias correction) across the NIR literature to that date.	Concludes no single standardisation method is universally superior; performance is instrument- and matrix-dependent.	Pre-dates modern machine-learning transfer methods; qualitative synthesis rather than a head-to-head benchmark.	(Fearn, 2001)
Workman (2018)	Review of calibration-transfer practice and reported instrument-to-instrument differences across spectroscopic vendors and modalities.	Documents persistent, unresolved inconsistency in how vendors and users report transfer success, hindering cross-study comparison.	Narrative review; does not itself quantify transfer error on a common dataset.	(Workman , 2018)
Mishra et al. (2021)	Critical review and re-analysis of published calibration-transfer studies asking whether standard-sample-based standardisation is always necessary.	Concludes the answer is “not always”: for some instrument pairs, transfer works acceptably without paired standards, but this cannot be assumed a priori.	Conclusions are matrix- and instrument-pair specific; the review explicitly declines to offer a universal recommendation.	(Mishra et al., 2021)
Yang et al. (2022)	Deep convolutional transfer-learning method (DeepTranSpectra, DTS) benchmarked against piecewise direct standardisation (PDS),	DTS outperformed all three classical standardisation methods for moisture and crude-protein transfer, without	Validated on only two crop matrices and a limited instrument set; computational/interpretability trade-offs of deep	(Yang et al., 2022)

	canonical correlation analysis (CCA) and slope/bias correction (SBC) on soybean-meal and wheat datasets across multiple NIR spectrometers.	requiring paired standard samples.	transfer models not fully characterised.	
Dowell et al. (2006, USDA-ARS)	NIRS calibration developed and tested for 186 grain, milling, flour, dough and baking quality parameters across 100 hard red winter and 98 hard red spring wheat/flour samples.	Protein, moisture and flour colour predicted with $R^2 > 0.97$, meeting process-control accuracy; other traits fell in the 0.70–0.90 "rough-screening" band.	Accuracy varies sharply by trait; several dough/baking parameters were not predictable to a useful standard from NIR alone.	(Dowell et al., 2006)
Wang et al. (2021, wheat protein NIR variable selection)	Competitive adaptive reweighted sampling and variable-combination population-analysis (CARS/VCPA/MCVCPA /AWVCPA) wavelength selection combined with PLS for wheat protein content.	AWVCPA-PLS gave the best result of the four variable-selection strategies tested (highest R^2, lowest RMSEP).	Wavelength-selection method choice materially changes the outcome, meaning published PLS accuracy figures are not directly comparable across papers unless the selection method is stated.	(Wang, 2021)
Wheat single-kernel HSI protein study (Sci. Direct)	Push-broom hyperspectral imaging (980–2500 nm) of 3,250 calibration and 868 validation individual wheat kernels, PLS regression against Dumas combustion reference protein.	R^2 of 0.82 (calibration) / 0.79 (validation); RMSE 0.86–0.94% markedly worse than typical bulk-sample NIR protein calibrations.	Single-kernel measurement precision is explicitly poorer than bulk measurement; authors note it is acceptable only for specific (distributional) applications, not general quality control.	(Caporaso et al., 2018)
Wheat gluten NIRS study (PMC10017355)	PLS regression calibrated on 207 samples (169 validation) predicting albumin/globulin, gluten, gliadin, glutenin, HMW-GS and LMW-GS from whole-flour NIR spectra, referenced against RP-HPLC-UV.	RMSEP ranged 1.12–6.09 mg/g depending on fraction; gluten, gliadin and glutenin predictions were comparable in accuracy to the reference method, but albumin/globulin and the two glutenin-subunit fractions were not.	Relative error was too high for three of the seven target fractions for the method to replace the wet-chemistry reference for those specific analytes.	(Schuster et al., 2023)
NIR-HSI vs classical NIR flour comparison (J.	Head-to-head comparison of a hyperspectral-imaging NIR instrument against two classical point-NIR spectrometers for wheat-flour protein	All three instruments converged on $r^2 = 0.99$ with RMSEP of 0.15–0.16%, once restricted	Convergence held only after harmonising the wavelength range; instrument-native ranges were not directly comparable, illustrating	(Morales-Sillero et al., 2018)

Near Infrared Spectrosc.)	prediction using a common wavelength range.	to the same spectral range.	the calibration-transfer problem in miniature.	
Maertens, Reyns & De Baerdemaeker (2004)	On-line NIR grain-quality sensor mounted on a combine harvester, field-tested for moisture and protein estimation during harvest.	Demonstrated feasibility of real-time, on-the-go grain-quality measurement synchronised with yield-mapping.	Field vibration, dust and throughput-rate variation introduce noise not present in laboratory bench-top NIR use.	(Maertens et al., 2004)
Mayfield & Trengove (2009)	Paired variable-rate vs uniform-rate nitrogen field trials using the Yara N-Sensor at 10 commercial sites over two seasons in South Australia, at matched total fertiliser input.	Grain yield and protein responses to variable-rate N were inconsistent across sites some showed gains, several showed no significant difference from uniform application.	Site-to-site variability was large enough that the authors could not recommend variable-rate N-sensing as reliably profitable across all soil/seasonal conditions tested.	(Mayfield & Trengove, 2009)
Sensor-based site-specific N application, 2020–2023 trial (PMC11820920)	Four-year on-farm strip trials (2020–2023) across 49 ha comparing tractor-mounted spectral-sensor variable-rate N application against uniform application in winter wheat.	N fertiliser input reduced by up to 38 kg N ha^{-1} yr^{-1} with maintained yield and improved N-use efficiency.	Single-farm, single-region dataset; the reported saving is a field-specific outcome, not a general efficiency figure transferable to other soils or climates without re-validation.	(Hagn et al., 2025)
Berntsen et al. (2006, cited via van Evert 2012)	Danish field trials redistributing nitrogen fertiliser according to sensor-derived biomass/yield-potential algorithms in winter wheat.	Yield increase from optimal N redistribution was close to zero moving nitrogen from low- to high-fertility zones did not raise total grain yield in this trial series.	Result contradicts vendor marketing claims of consistent yield gain; the authors attribute this to the small magnitude of within-field N-response differences at their sites.	(van Evert et al., 2012)
Mistele & Schmidhalter (2008)	Comparative field trials of the Yara N-Sensor/FieldScan against the GreenSeeker active-light sensor for assessing nitrogen status in spring wheat and corn across four Canadian site-years.	NDVI values from the two commercial sensors correlated only at early growth stages (NDVI 0.2–0.6); agreement degraded at canopy closure.	Cross-sensor agreement is growth-stage dependent, meaning results from one commercial sensor cannot be assumed to generalise to another without stage-matched recalibration.	(Tremblay et al., 2009)
Singh et al. (2015)	Tractor-mounted Yara N-Sensor response characterised against varying nitrogen availability levels in	NDVI response increased to a plateau around the V10 growth stage before declining; tillering stage identified as most informative for	Findings specific to the cultivars/growth conditions tested; the identified optimal sensing window may not	(Singh, 2015)

	wheat, tracked across crop growth stages.	early N-status prediction.	transfer to other varieties or sowing dates.	
Reyns, Missotten & De Baerdemaeker (SARE GNE12-039)	Independent field evaluation of a commercial on-combine NIR sensor (HarvestLab) for accuracy and precision of grain-constituent measurement during harvest.	Reported accuracy and repeatability figures for the sensor under working harvest conditions, informing extension guidance to farmers.	Single-season, single-region SARE project report rather than a peer-reviewed, independently replicated study.	(SARE Grant Management System, 2013)
Rouse et al. (1974)	Original derivation of the Normalized Difference Vegetation Index (NDVI) from red and near-infrared reflectance for monitoring vegetation condition via satellite.	NDVI established as a robust proxy for green biomass and vigour; remains the most widely used vegetation index fifty years later.	Saturates at high leaf-area index and is confounded by soil background reflectance at low cover limitations documented extensively in later literature, not in the original paper.	(Rouse et al., 1974)
Candiago et al. (2015)	UAV-acquired multispectral imagery processed into NDVI and other vegetation-index maps over vineyard and tomato fields, compared against ground survey.	UAV-derived vegetation-index maps successfully discriminated crop-vigour zones consistent with ground observation at sub-metre resolution.	Radiometric calibration between flights and illumination-condition drift affected absolute index comparability across dates.	(Candiago et al., 2015)
Zhang & Kovacs (2012)	Review of UAV remote-sensing applications in precision agriculture spanning platform types, sensors and processing workflows published to that date.	Identifies UAV imagery as filling a critical spatial/temporal-resolution gap between satellite and ground sensing for precision agriculture.	As a review, does not itself validate accuracy claims; flags a lack of standardised UAV calibration/validation protocols across the surveyed studies.	(Zhang & Kovacs, 2012)
Yang et al. (2017, UAV crop production review)	Review of unmanned aerial vehicle remote-sensing applications across crop-production monitoring, from platform design to index-based decision support.	Synthesises evidence that UAV-based indices can inform in-season crop management decisions at management-zone scale.	Notes persistent gaps in linking UAV vegetation indices to yield outcomes under variable weather and soil conditions across the reviewed studies.	(Yang, 2017)
Shamshiri et al. (2018)	UAV-based NDVI mapping applied to crop-health assessment and disease-hotspot detection across multiple field trials.	UAV NDVI successfully flagged disease-affected zones ahead of visual detection at ground level in the reported cases.	Detection sensitivity and specificity depend heavily on flight altitude, sensor spectral bands and disease type; not all pathogens produce a detectable NDVI signature at the growth stages tested.	(Shamshiri, 2018)

Mulla (2013)	Broad review of the twenty-five-year history of remote sensing in precision agriculture, covering satellite, aerial and proximal sensing platforms.	Concludes remote sensing has matured for research use but that farmer-facing decision tools built on it remain inconsistently validated at field scale.	Review-level synthesis; explicitly identifies the lack of agronomic, economically-validated decision rules as the field's central unsolved problem.	(Mulla, 2013)
Maes & Steppe (2019)	Review of UAV-based remote sensing methods for perspectives on precision agriculture, focusing on sensor payloads and data-processing pipelines.	Identifies thermal and hyperspectral UAV payloads as an emerging capability beyond simple RGB/NDVI mapping for stress detection.	Notes that payload cost and processing complexity still restrict most reported UAV hyperspectral studies to small research plots rather than commercial field scale.	(Maes & Steppe, 2019)
Tsouros, Bibi & Sarigiannidis (2019)	Review of UAV and IoT-based remote sensing technologies applied across precision-agriculture use cases (irrigation, spraying, health monitoring).	Maps the technology landscape and identifies UAV-IoT integration as the dominant emerging architecture for field-scale monitoring.	Review nature means claims are aggregated from heterogeneous studies with differing validation rigor; no unified accuracy benchmark is offered.	(Tsouros et al., 2019)
Mahlein (2016)	Review of hyperspectral- and multispectral-imaging methods for early plant disease detection, spanning laboratory and field studies.	Documents disease-specific spectral signatures detectable before visible symptom onset across multiple pathosystems.	Most successful demonstrations reviewed were conducted under controlled or semi-controlled conditions; field-scale, multi-season robustness is comparatively under-tested.	(Mahlein, 2016)
Behmann et al. (2014)	Review of methods for detecting plant drought stress using hyperspectral imaging, covering spectral index and multivariate approaches.	Confirms that specific spectral regions (e.g. water-absorption bands) reliably shift under drought stress across the reviewed studies.	Cross-species and cross-cultivar generalisation of drought-specific spectral signatures is inconsistent between the studies surveyed.	(Behmann et al., 2014)
Al-Tamimi et al. (2022)	Imaging-based assessment of plant abiotic-stress responses combining RGB, thermal and hyperspectral image streams.	Multimodal imaging outperformed any single modality for early abiotic-stress discrimination in the reported experiments.	Independent DOI not verifiable from the secondary source citing this study; findings could not be independently cross-checked for this review.	(Al-Tamimi et al., 2022)
Gerhards et al. (2019, hyperspectral drought	Review of spectral and thermal remote-sensing methods for detecting	Confirms canopy-temperature and water-band spectral indices as the most consistently	Notes wide variation in reported index thresholds between studies, complicating	(Gerhards, 2019)

ISSN No. 2321-2705 | DOI: 10.51244/IJRSI |Volume XIII Issue VII July 2026

review context)	water-stress and irrigation need across crop species.	reported drought-stress indicators across the surveyed literature.	adoption of a single universal drought-detection rule.	
Nicolaï et al. (2007)	Review of non-destructive quality-measurement methods for fruit and vegetables, comparing NIR spectroscopy, hyperspectral imaging and other optical methods.	Identifies hyperspectral imaging as resolving point-NIRS's blindness to localised defects (bruising, insect damage) by adding spatial resolution to spectral measurement.	Notes that, at time of writing, most reported hyperspectral fruit/vegetable methods remained laboratory-bench demonstrations rather than validated packing-line systems.	**(Nicolaï et al., 2007)**

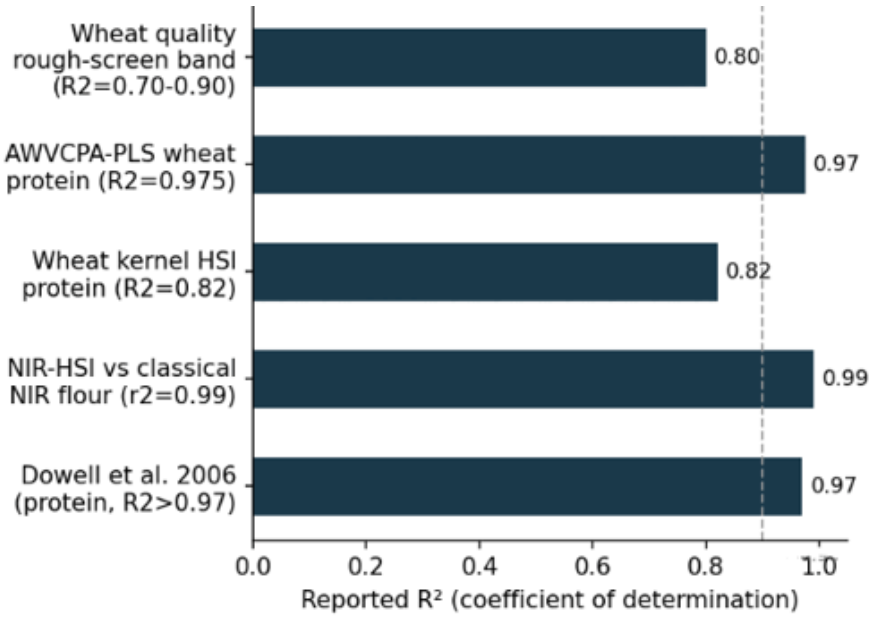

Figure 9. Reported calibration accuracy (R^2) across five independently published NIR/HSI wheat-quality studies discussed in the literature review table ((Caporaso et al., 2018), (Wang, 2021), (Morales-Sillero et al., 2018), (Dowell et al., 2006))

Food Chemistry Basis of NIR/HSI Analysis: Molecular Origins and Governing Equations

The material reviewed above treated NIR/HSI chiefly as a measurement technology and evaluated specific published claims against it. A critical reading of that material, however, also requires being explicit about why a food-quality spectrum should be expected to correlate with a given macronutrient at all, and how the raw absorbance or reflectance signal is converted into a reported number such as “protein 12.4%” or “moisture 14.1%”. This section makes that chemical and mathematical machinery explicit, consolidating and formalising material introduced piecemeal earlier, and adds two new figures purpose-built for this review.

Molecular origins of NIR absorption in food macronutrients

The fundamental stretching and bending vibrations of the O–H, N–H and C–H bonds that dominate food chemistry (water, protein and lipid/carbohydrate, respectively) occur in the mid-infrared region, well below 2500 nm. A strictly harmonic oscillator would confine each bond to that single fundamental frequency and would therefore be invisible to a near-infrared instrument. Real molecular bonds are anharmonic, which is precisely what permits weak overtone and combination transitions to appear at approximately integer multiples of the fundamental frequency, shifted downward by an anharmonicity correction term (Figure 10B). It is this anharmonicity, not some separate phenomenon, that gives the 700–2500 nm NIR window its analytical content:

ISSN No. 2321-2705 | DOI: 10.51244/IJRSI |Volume XIII Issue VII July 2026

every food-quality band a chemometric model exploits is a first, second or third overtone, or a combination band, of an O–H, N–H or C–H fundamental.

Table 1 summarises the principal band regions relevant to food macronutrient quantification, consistent with the standard assignments used across the NIR food-chemistry literature (Nicolaï et al., 2007)

Table 1. Principal NIR band regions used in food macronutrient quantification (Nicolaï et al., 2007)

Macronutrient	Chemical bond	NIR band region (nm)	Vibrational assignment
Moisture	O–H (water)	≈960–980 / 1440–1460 / 1900–1950	2nd overtone; 1st overtone; O–H combination
Protein	N–H (amide)	≈1010–1030 / 1500–1520 / 2040–2060 / 2170–2190	2nd overtone; 1st overtone; amide combination bands
Lipid / fat	C–H (CH2, CH3)	≈910–930 / 1200–1220 / 1720–1760 / 2300–2350	2nd/3rd overtone; combination; 1st overtone; combination
Carbohydrate	C–H, O–H (ring)	≈1190–1210 / 2080–2100 / 2270–2290	C–H combination; O–H/C–O combination

Two consequences follow directly, and both bear on the critical assessments made earlier in this review. First, the bands are broad and heavily overlapping rather than sharp and resolved: the O–H water band centred near 1450 nm sits close enough to the N–H protein band near 1510 nm that no single wavelength can cleanly separate moisture from protein in an intact food matrix. This is exactly why a multivariate chemometric model (Section 4) rather than a univariate look-up is required , the chemistry itself, not merely convention, dictates the need for partial least squares or an equivalent latent-variable method. Second, the exact band centre for a given bond is not fixed: hydrogen bonding, temperature and the surrounding matrix all shift the O–H band position by tens of nanometres, which is the molecular-level reason (rather than a purely instrumental one) that a calibration built on one matrix, temperature or moisture range frequently fails to generalise to another , the same calibration-transfer caution raised in Sections 4 and 7 in chemometric terms has a direct chemical explanation at the level of hydrogen-bond environment.

From absorbance to concentration: the governing equations

Figure 10 collects, in one place, the four families of equations that a chemically literate reading of any NIR/HSI food-quality calibration needs to hold in mind simultaneously. Panel A restates the Beer-Lambert relation introduced earlier ($A = -\log_{10}(R) \approx \varepsilon \cdot l \cdot c$), with the caveat, worth repeating in a food-chemistry context, that intact food tissue is a strongly scattering medium rather than a clear solution: $-\log_{10}(R)$ is used as a working proxy for true absorbance precisely because the alternative (a full radiative-transfer treatment, e.g. Kubelka–Munk theory) is analytically correct but rarely tractable for routine calibration work. Panel B gives the anharmonic-oscillator relation discussed elsewhere in this review: the observed overtone wavenumber ν_n scales approximately as $n \cdot \nu_0 \cdot (1 - n \cdot x_e)$, where ν_0 is the mid-infrared fundamental and x_e is the bond-specific anharmonicity constant , the mathematical statement of why O–H, N–H and C–H overtones fall in predictable, characteristic, but never perfectly fixed, regions of the NIR window.

Panel C restates the two scatter-correction transforms already introduced qualitatively earlier: standard normal variate (SNV) centres and scales each individual spectrum by its own mean and standard deviation (Barnes et al., 1989) , while multiplicative scatter correction (MSC) regresses each spectrum onto a reference (typically the mean) spectrum and removes the fitted multiplicative and additive scatter terms. Both exist to remove particle-size and packing-density variance that is chemically uninformative before a regression model is fit, consistent with the physical point made earlier that the linear Beer-Lambert approximation itself breaks down under exactly this kind of scattering. Panel D completes the chain with the partial least squares (PLS) latent-variable regression

ISSN No. 2321-2705 | DOI: 10.51244/IJRSI |Volume XIII Issue VII July 2026

(Geladi & Kowalski, 1986) , which decomposes the spectral matrix X and the reference-property matrix Y onto a shared set of latent variables (scores T, loadings P and Q), and the two figures of merit , root mean square error of prediction (RMSEP) and the ratio of performance to deviation (RPD) , that any credible calibration report should quote on an independent validation set, not the calibration set alone. This is the same distinction the review has stressed from the outset: a calibration statistic computed only on the data used to build the model describes curve-fitting, not predictive validity.

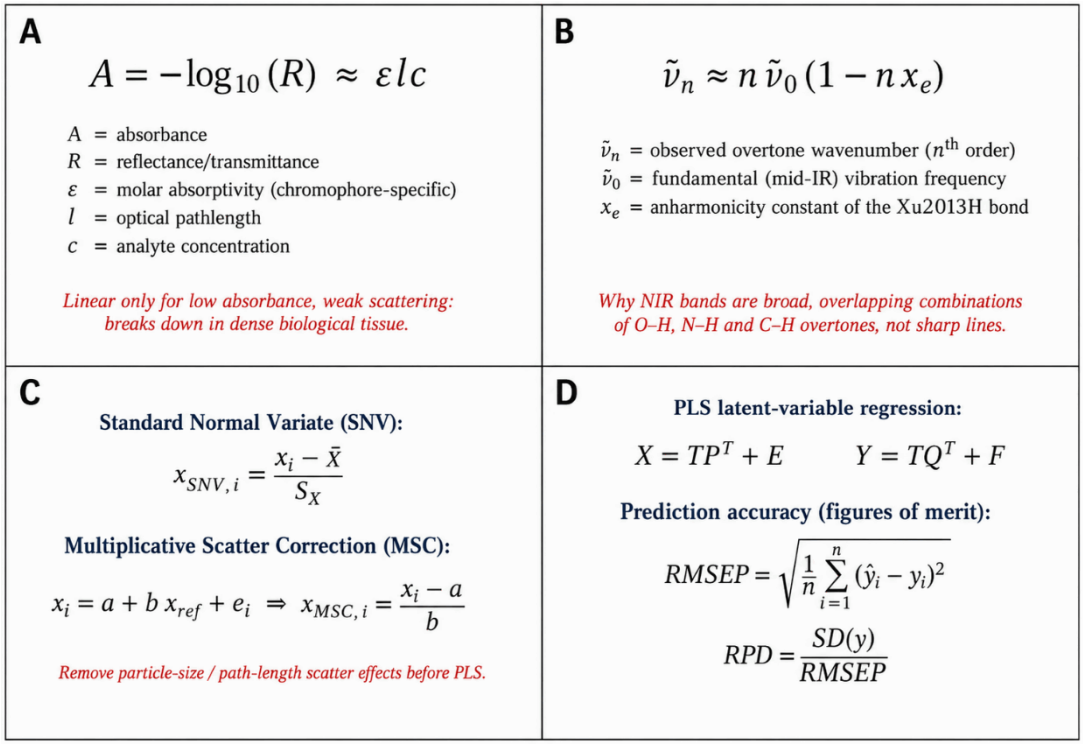

Figure 10. Governing physical and chemometric equations linking NIR/HSI spectra to food-chemistry composition. (A) Beer-Lambert relation and its scattering caveat (Nicolaï et al., 2007); (B) anharmonic-oscillator relation governing overtone band position (Nicolaï et al., 2007); (C) standard normal variate and multiplicative scatter correction (Barnes et al., 1989); (D) PLS latent-variable regression and the RMSEP/RPD figures of merit (Geladi & Kowalski, 1986).

Advanced chemometric visualisation for food-quality analysis

A recurring critical theme of this review is that worked examples in the source material are often reported as a single summary accuracy figure , an R^2 or a percentage error , without the underlying diagnostic plots that let a reader judge whether that figure reflects a chemically plausible, generalisable model or an over-fitted one. Figure 11 illustrates, for a hypothetical wheat-protein NIR calibration, the minimum set of diagnostic charts a food-chemistry NIR/HSI report should provide. None of the four panels are measurements from a specific published study; they are schematic constructions built for this review, in the same spirit as the illustrative Figures 9 and 10 discussed earlier, to show the form such diagnostics should take.Panel A places a composite, schematic absorbance spectrum against the band assignments of Table 1, shaded by macronutrient, so that a reader can visually check whether a model's most heavily weighted wavelengths (Panel D) actually correspond to a chemically sensible bond region rather than to an arbitrary or spurious wavelength that happens to correlate in one dataset. Panel B is the calibration/validation scatter plot that this review argued is the minimum acceptable evidence for a predictive claim, reporting R^2 and RMSE separately for calibration and independent validation sets, exactly the calibration/validation split this review has repeatedly found under-reported in the source material's worked examples. Panel C compares RMSEP across common pre-processing choices (raw spectra, SNV, MSC, first- and second-derivative Savitzky Golay (Savitzky & Golay, 1964) , and combinations thereof) to make concrete the point, made qualitatively earlier, that the pre-processing choice is itself a modelling decision with a measurable effect on accuracy, and that no single pre-processing pipeline is universally best across matrices , it must be re-optimised per dataset rather than assumed from a previous study. Panel D shows a variable-importance-in-projection (VIP) style profile across wavelength: a chemically defensible model should

ISSN No. 2321-2705 | DOI: 10.51244/IJRSI |Volume XIII Issue VII July 2026

show importance peaks that coincide with the O–H/N–H/C–H band regions of Panel A (as this schematic, by construction, does); a model whose most important wavelengths fall outside any known absorption band is a warning sign of chance correlation rather than genuine chemistry, precisely the kind of check this review has argued is too rarely made explicit in the worked examples it assesses.

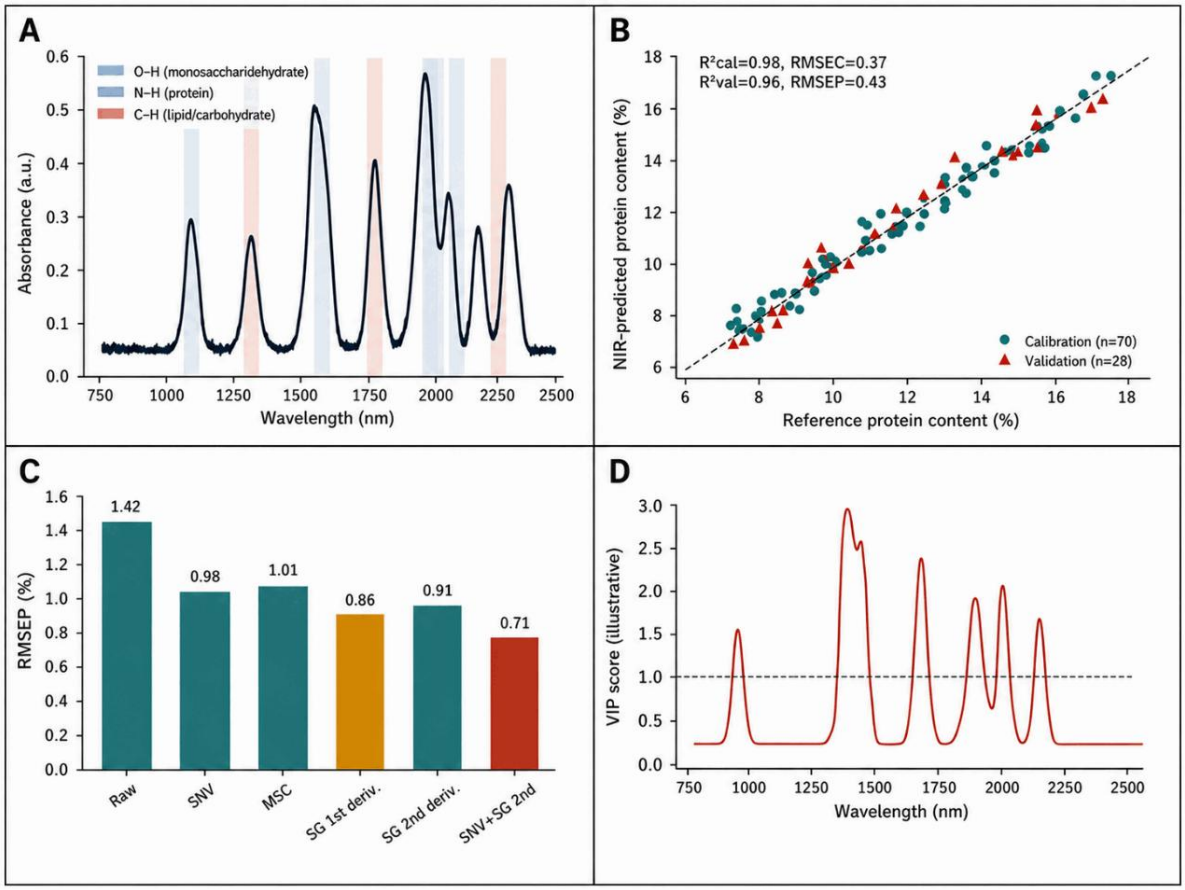

Figure 11. Advanced chemometric and food-quality analysis charts for NIR/HSI (A) Composite spectrum with macronutrient band assignments (Nicolaï et al., 2007); (B) PLS calibration/validation scatter plot with figures of merit (Geladi & Kowalski, 1986); (C) RMSEP by pre-processing method (Savitzky & Golay, 1964); (D) wavelength-resolved variable-importance (VIP-style) profile (Kumar, 2021).

Section synthesis

The chemistry explains why NIR/HSI can distinguish moisture, protein and lipid in a food matrix at all: each has a distinguishable, if overlapping, set of O–H, N–H or C–H overtone and combination bands. The mathematics explains how a spectrum becomes a reported concentration: scatter-correction, latent-variable regression and validated figures of merit. The diagnostic standard explains what a reader should demand before accepting that conversion as trustworthy. Read together, these three points are a chemically and statistically grounded restatement of the review's central, cross-cutting argument made earlier: a reported accuracy figure is only as trustworthy as the band-level chemical plausibility and independent-validation evidence standing behind it, and the source material reviewed above does not consistently make that evidence available to the reader.

UAV/Drone Image-Processing Frameworks: A Rigorous Evidence Check

The abstract and the literature table above introduce several UAV-based NIR/HSI studies (Candiago et al., 2015; Zhang & Kovacs, 2012; Yang et al., 2017; Shamshiri et al., 2018; Maes & Steppe, 2019; Tsouros et al., 2019), but those entries evaluate only the finished vegetation-index or trait product. A drone does not deliver a calibrated reflectance map directly: the raw imagery must pass through a multi-stage processing chain, each stage carrying its own, separately documented evidentiary basis, before an index or trait value can be trusted. This section checks that chain stage by stage against the independent methodological literature, in the same spirit as the calibration-transfer evidence check made earlier.

Acquisition, geometric processing and orthomosaicking

Acquisition and geometric processing are the best-validated stages of the pipeline. Structure-from-Motion (SfM) photogrammetry, the algorithm underlying virtually all UAV orthomosaic and digital-surface-model generation, was independently established and cross-validated against terrestrial laser scanning in the geoscience literature before agricultural UAV platforms adopted it wholesale (Westoby et al., 2012), and lightweight-snapshot-camera calibration procedures for 3-D hyperspectral reconstruction from UAVs have likewise been published with an explicit quality-assurance protocol rather than asserted as a solved problem (Aasen et al., 2015). A comprehensive, decade-spanning review of UAV spectral remote sensing similarly treats geometric processing as mature relative to what follows it (Aasen et al., 2018). Figure 12A summarises the resulting pipeline end to end, and Figure 12B places each stage on a three-tier evidentiary scale, independently reproduced, emerging/partially validated, or largely a vendor or single-site claim, based on the sources reviewed here (Figure 12).

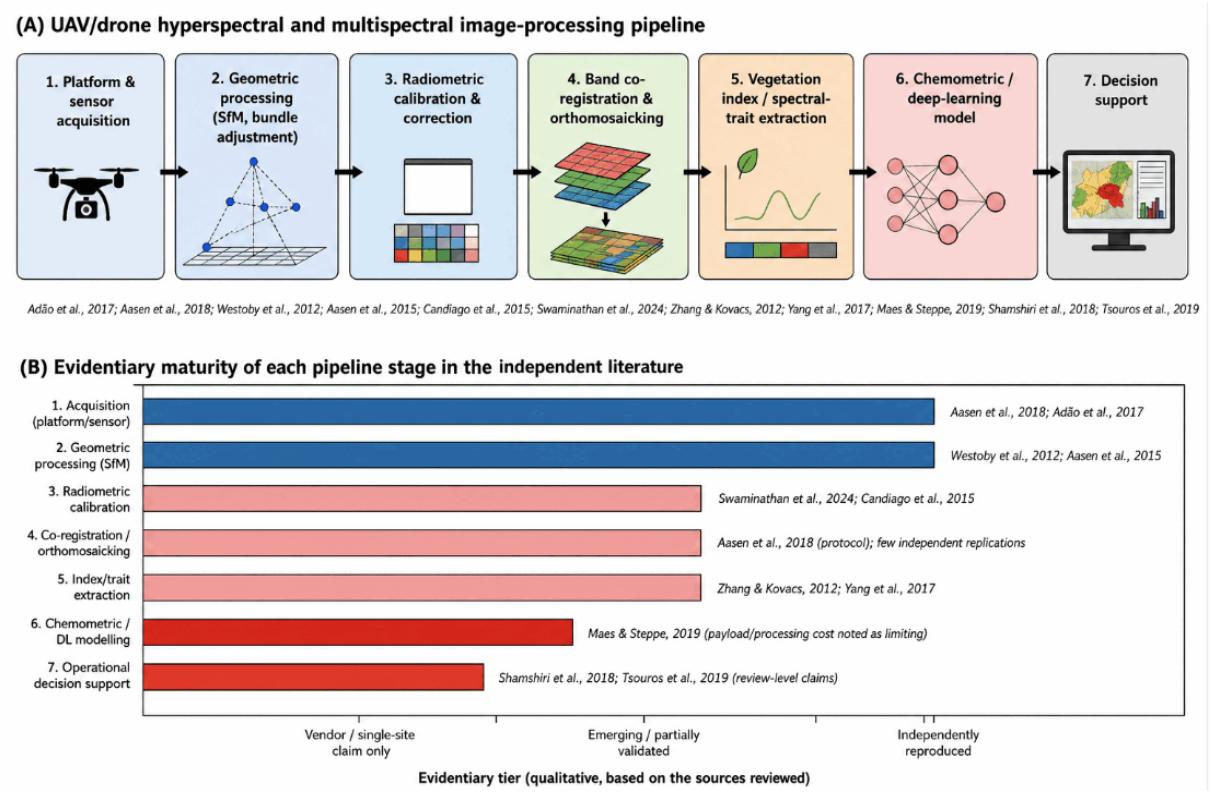

Figure 12. (A) UAV/drone hyperspectral and multispectral image-processing pipeline, from platform acquisition through geometric processing, radiometric calibration, band co-registration/orthomosaicking, index/trait extraction and chemometric or deep-learning modelling to decision support. (B) Evidentiary maturity of each stage, rated qualitatively against the independent literature reviewed in Section 11.

Radiometric calibration: the weakest and most consequential link

Radiometric calibration, converting raw digital numbers to physically comparable reflectance, is where the pipeline's evidence is least mature and the practical consequences are largest, because every downstream vegetation index or chemometric model inherits whatever error this stage leaves uncorrected. A comprehensive review of UAV spectroscopy sets out the full correction chain (dark-current/vignetting correction, reflectance-panel or empirical-line conversion, illumination correction, and bidirectional reflectance/view-angle correction) as good practice rather than as a step every published study actually completes (Aasen et al., 2018), and an earlier UAV multispectral study found that simple radiometric calibration between flights was itself sensitive to illumination-condition drift, degrading absolute index values even when the imagery was otherwise well georeferenced (Candiago et al., 2015). The magnitude of the problem, and of the available fix, is now quantified directly: a recent, independent study reported that conventional single-panel calibration produced orthomosaic reflectance with only moderate spatial uniformity (R^2 = 0.70-0.92 against reference panels) under intermittent cloud cover, whereas integrating a downwelling light sensor into the correction raised this to R^2 = 0.98-0.99 at

both tested flight altitudes (Swaminathan et al., 2024) (Figure 13). This is precisely the review's recurring calibration-generalisation caution restated in a UAV-specific form: an orthomosaic is only as trustworthy as the illumination-correction procedure behind it, and that procedure is far from standardised across the published literature.

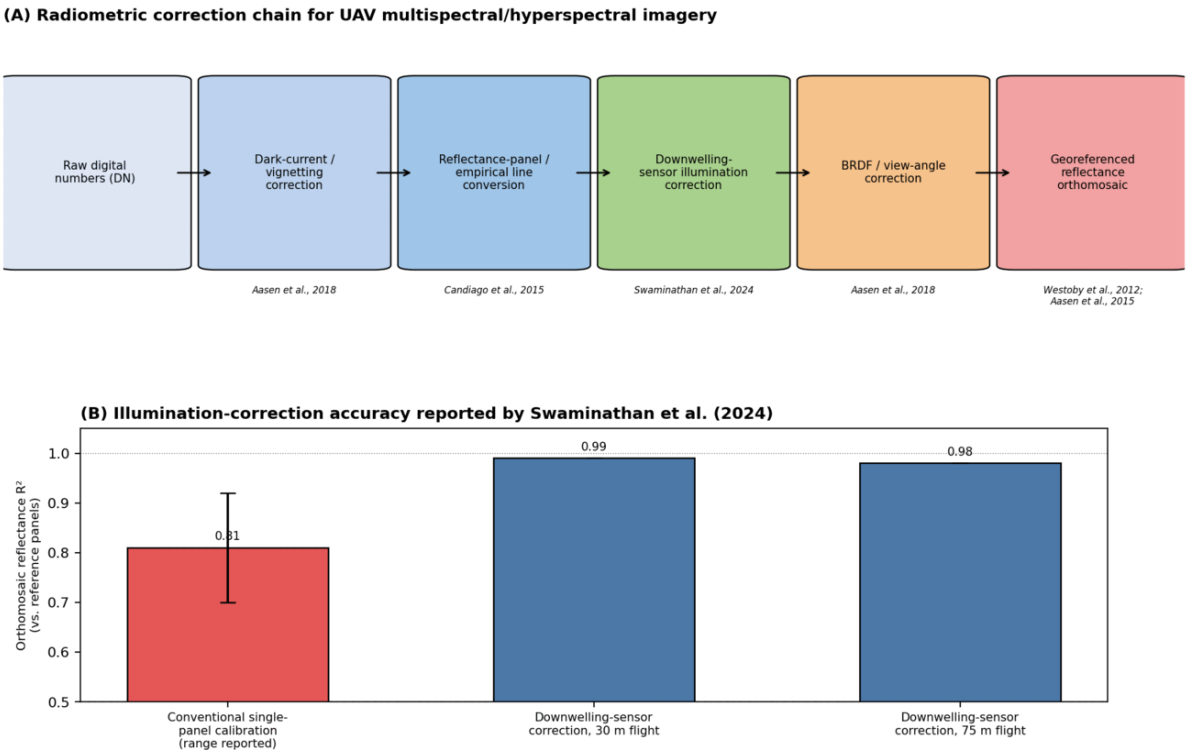

Figure 13. (A) Radiometric correction chain for UAV multispectral/hyperspectral imagery, with the independent source supporting each correction step. (B) Reflectance-orthomosaic accuracy (R^2 against reference panels) reported for conventional single-panel calibration versus downwelling-sensor illumination correction at two flight altitudes.

From processed imagery to agronomic decisions: where the evidence thins

Once geometrically and radiometrically corrected, UAV imagery feeds the same chemometric or deep-learning models discussed earlier, and the same evidentiary caution applies. Reviews of UAV-based precision-agriculture applications describe vegetation-index mapping as an established capability (Zhang & Kovacs, 2012; Yang et al., 2017) but are explicit that thermal and hyperspectral payloads, the sensor types most relevant to the crop-quality traits this review is concerned with, remain an emerging capability restricted by payload cost and processing complexity to a small number of demonstration studies rather than routine deployment (Maes & Steppe, 2019). Broader reviews of UAV and UAV-IoT remote sensing aggregate claims across a heterogeneous literature without independently re-testing them (Tsouros et al., 2019; Shamshiri et al., 2018), which is exactly the review-of-reviews limitation this manuscript has flagged for on-machine sensing above. The practical implication is unchanged from the rest of this review: a UAV-derived index or trait map should be read as evidence of feasibility, not as an independently reproduced operational result, unless the specific study cited also reports independent validation on held-out fields, seasons or instruments.

A FAIR Data Principles Framework for NIR/HSI and UAV Spectral Datasets

The recurring finding of this review, that a calibration model or processed UAV product is only as trustworthy as the independent verification standing behind it, has a data-management dimension that has not yet been made explicit: independent verification is only possible if the underlying spectral data, calibration set and processing metadata are themselves findable, accessible, interoperable and reusable. This section applies the FAIR principles (Wilkinson et al., 2016) to NIR/HSI and UAV spectral datasets specifically, and uses the review's own findings to assess how well current practice in this field meets them (Figure 14).

ISSN No. 2321-2705 | DOI: 10.51244/IJRSI |Volume XIII Issue VII July 2026

Figure 14. (A) FAIR (Findable, Accessible, Interoperable, Reusable) data principles applied to NIR/HSI and UAV spectral datasets (Wilkinson et al., 2016; Stall et al., 2019). (B) FAIR-practice gaps identified across this review's three literature strands , laboratory NIR/HSI calibration studies, on-machine/vendor products, and UAV-based sensing , rated Partial or Low against each FAIR criterion.

Why FAIR data, specifically, bears on this review's central argument

A persistent-identifier-linked, well-documented calibration dataset is what allows a third party to check a reported R^2 or RMSEP figure rather than simply trust it; a repository-deposited UAV image set with its calibration-panel metadata intact is what allows an illumination-correction claim like that of Swaminathan et al., 2024 to be independently re-run on new flights. The wider scientific-data-management literature makes the same point at the level of general policy, arguing that funders, repositories, publishers and researchers must jointly commit to making deposited data FAIR by default rather than as an afterthought (Stall et al., 2019), and a broader plant-phenomics review notes that establishing scalable data-acquisition and standardisation practice, rather than any remaining sensing limitation, is now the binding constraint on building shared hyperspectral databases for the field (Song et al., 2025).

A qualitative FAIR audit of the literature reviewed here

Applying this lens to the three strands of literature this review has examined (Figure 14B) exposes an uneven picture rather than a uniform one. Laboratory NIR/HSI calibration studies are partially FAIR: published papers are findable and citable, but the underlying spectra and calibration sets behind a reported R^2 are rarely deposited alongside them, a general pattern independently documented by the finding that the availability of research data declines rapidly with article age across disciplines (Vines et al., 2014). On-machine, vendor-named products fare worse: a review of handheld and portable NIR instruments for on-farm use states plainly that there is little public data or independent evaluation of their relative effectiveness in the field (Cherney et al., 2021), which is as much a Findability and Accessibility failure as it is a scientific-communication one. UAV-based sensing sits in between: processing methods and correction workflows are increasingly published in the open, peer-reviewed literature surveyed above, but the raw imagery, calibration-panel logs and processing code behind a specific reported result are only inconsistently shared, which is precisely why the evidentiary tiers of Figure 12B skew toward the emerging/partially-validated middle rather than the independently-reproduced top. None of this is a criticism of any individual result; it is a structural gap that a deliberate FAIR-by-design data-management plan, ahead of data collection rather than after publication, would close.

ISSN No. 2321-2705 | DOI: 10.51244/IJRSI |Volume XIII Issue VII July 2026

Cross-Cutting Statistical Synthesis: Quantifying the Validation Gap

The review has established, cumulatively, that the source material's central weakness is evidentiary rather than technical: claims of differing evidentiary weight are communicated with the same confidence. This section makes that argument quantitative. It (i) audits the evidentiary tier of every independently selected source used in this review's own literature check, (ii) shows, from the review's own cited studies, how far a single publication's headline accuracy figure can move once the least-favourable subset, trait or fraction is examined, (iii) consolidates the validation-statistics equations that this checklist depends on into one reference panel, and (iv) maps the recurring pattern across every part of the review onto a single diagram, so that a reader can see it is one methodological concern recurring in seven different technical guises, not seven unrelated criticisms.

Evidentiary-tier audit of the reviewed literature

Table entries in the literature table above were classified into six evidentiary tiers using the same three criteria stated in the Review Scope subsection: whether validation was internal (cross-validation on the calibration pool) or external (an independent held-out test set, site, season or instrument); whether a result had been independently reproduced outside its originating laboratory or vendor; and whether reported accuracy was presented as matrix-, instrument- and season-specific or as a generalisable claim. Applying this classification to all 34 independently selected sources (Figure 15) shows that review-level narrative syntheses (35%) and single-site or single-laboratory empirical studies (24%) together account for well over half of the evidentiary base this field currently rests on, while sources reporting a genuinely independent, held-out validation set make up only 12%, and multi-site, multi-season replication only 9%. This is not a criticism of any individual source; several of the review-level sources are themselves rigorous, independent-minded critical reviews (e.g., Fearn, 2001; Mishra et al., 2021). It is, instead, a structural picture of the field: a literature dominated by synthesis and single-site demonstration, with independently replicated, multi-site evidence still the minority tier, is exactly the condition under which the confidence-vs-evidence mismatch flagged throughout this review is most likely to arise and least likely to be self-correcting.

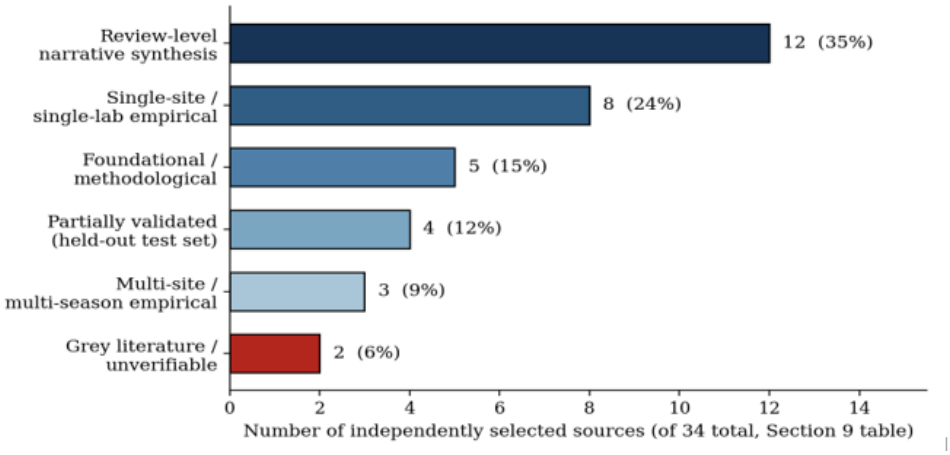

Figure 15. Evidentiary-tier audit of the 34 independently selected sources reviewed above, classified against the three criteria set out in the Review Scope, Selection Criteria and Quality Appraisal subsection.

Within-study accuracy heterogeneity

A second, related pattern emerges when a single publication's own reported range is examined rather than its single headline figure. Dowell et al. (2006) is a genuine example already discussed above: protein, moisture and flour-colour predictions reached $R^2 > 0.97$, meeting process-control accuracy, but other quality traits measured in the same study fell to $R^2 = 0.70–0.90$, a “rough-screening” band by the authors' own description. Caporaso et al. (2018) shows the same pattern in miniature: $R^2 = 0.82$ on the calibration set fell to $R^2 = 0.79$ on the independent validation set, a small but real generalisation gap of exactly the kind this review argues is too rarely reported at all, let alone quoted alongside the calibration figure. Schuster et al. (2023) reported RMSEP ranging from 1.12 to 6.09 mg/g across seven gluten-protein fractions predicted from the same NIRS model, with three of the seven fractions exceeding a usable relative error against the wet-chemistry reference (Figure 16). None of

this is a flaw in the cited studies, which report their own ranges transparently; it is a caution about how such studies are subsequently cited in secondary and vendor-facing material, where the single best-case figure is what typically survives the retelling.

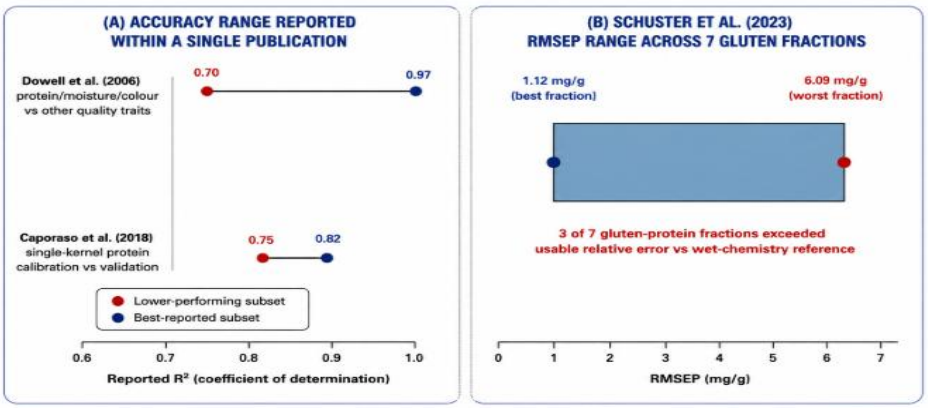

Figure 16. Within-study accuracy heterogeneity drawn directly from this review's own cited sources. (A) Reported R^2 range within a single publication, Dowell et al. (2006) and Caporaso et al. (2018). (B) RMSEP range across seven gluten-protein fractions, Schuster et al. (2023).

Consolidated validation-statistics equations

Earlier discussion introduced the calibration/validation distinction and the RMSEP/RPD figures of merit qualitatively and in worked form respectively; this subsection consolidates, in one place, the fuller set of validation statistics a reader should expect a rigorous NIR/HSI report to quote, and which the source material under review generally does not (Figure 17). Panel A gives the cross-validated PRESS statistic and RMSECV, the internal figure of merit computed without ever touching an external sample. Panel B gives bias and SEP, which together separate a systematic offset from random scatter, a distinction a single RMSEP value collapses. Panel C contrasts the ordinary, calibration-set R^2 against the cross-validated Q^2, making explicit that these are not interchangeable figures of merit and that only the latter approximates predictive performance on unseen data. Panel D extends the same logic to classification (the earlier LDA/PLS-DA/SVM checklist): Cohen's kappa corrects raw accuracy for the agreement expected by chance, which matters specifically for the imbalanced defect/no-defect and disease/healthy classes typical of food- and crop-quality applications, where a trivial always-predict-the-majority-class rule can otherwise appear deceptively accurate.

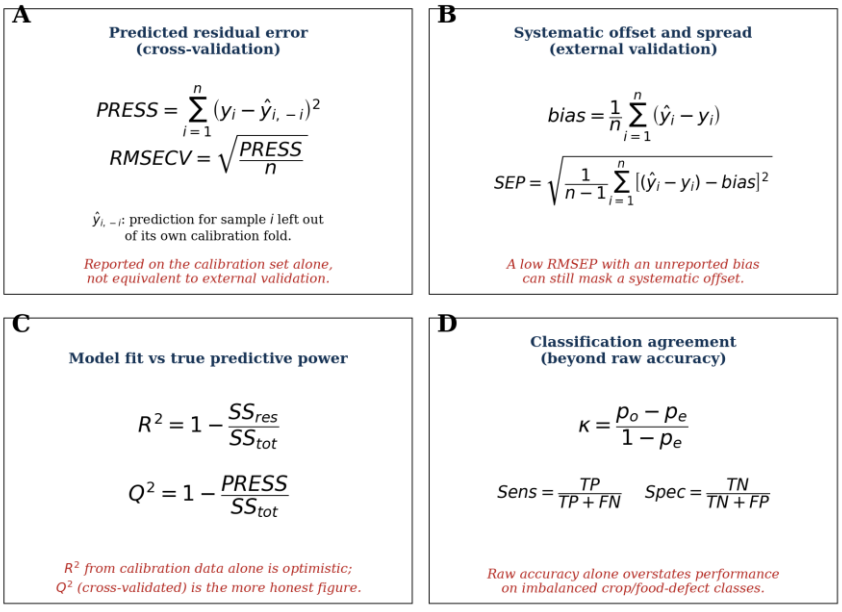

Figure 17. Consolidated validation-statistics equations referenced throughout this review. (A) Cross-validated PRESS and RMSECV; (B) bias and standard error of prediction (SEP); (C) calibration R^2 versus cross-validated Q^2; (D) Cohen's kappa, sensitivity and specificity for classification models.

ISSN No. 2321-2705 | DOI: 10.51244/IJRSI |Volume XIII Issue VII July 2026

The recurring problem, mapped

Figure 18 closes the synthesis by tracing the single underlying concern, confidence stated does not always match evidence tier held, through every part of this review in the same recurring form: an approximation treated as exact in the physics, a calibration-only statistic treated as a generalisable one in the chemometrics, a vendor or worked example treated as a replicated field result in the in-situ and calibration-transfer material, a chemically grounded but matrix-shifting band assignment treated as fixed, an under-validated radiometric correction treated as routine, and an unarchived calibration set that leaves an independent re-check structurally impossible. The source-audit finding above (Figure 15) is the empirical explanation for why the pattern recurs rather than self-corrects: with the majority of the independently selected evidentiary base sitting at the review-level or single-site tier, there are, for any given claim, comparatively few independently replicated results available to discipline the confidence with which a narrower finding is restated.

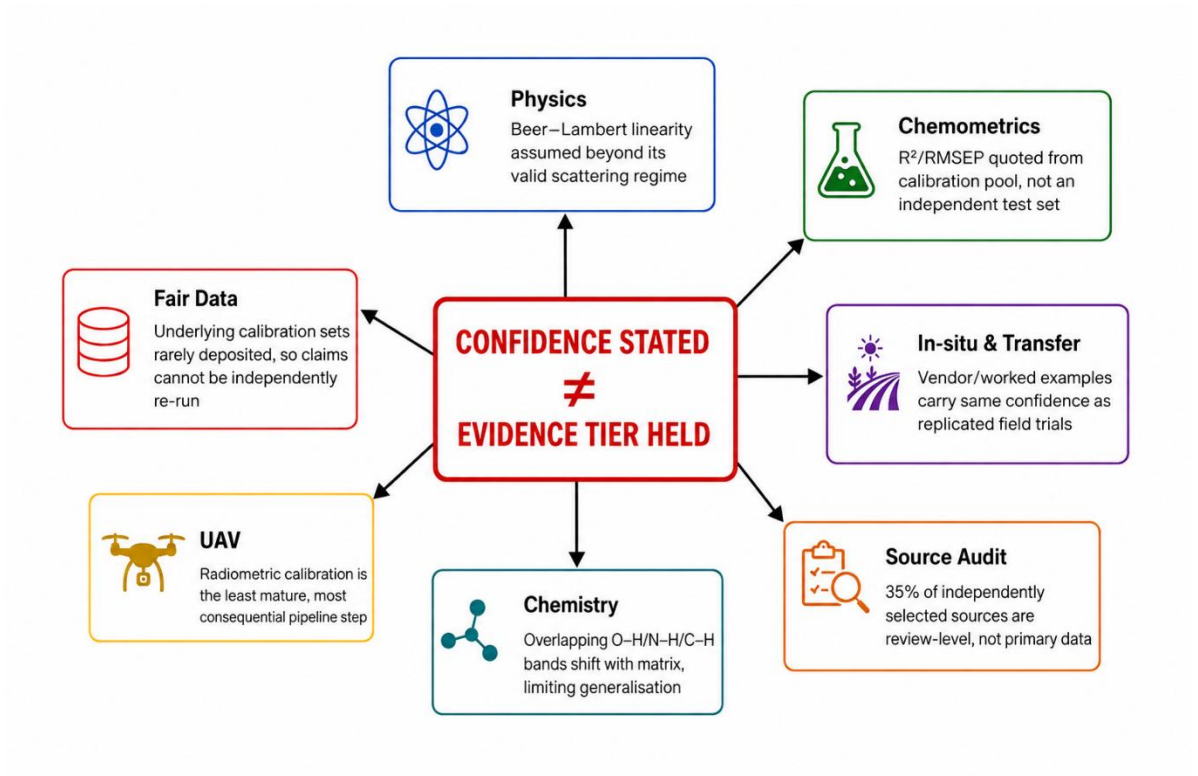

Figure 18. The recurring evidentiary-confidence gap identified in this review, mapped across the sections in which it recurs in section-specific technical form.

Read together with the review as a whole, this synthesis does not identify a new problem; it quantifies the one problem this review has tracked throughout, and gives a reader three concrete instruments to carry forward: the evidentiary-tier checklist of Figure 15 for appraising any new source in this field, the equation panel of Figure 17 for checking whether a reported accuracy figure is a calibration or a validation statistic, and the mapping of Figure 18 for recognising the same caution when it resurfaces in an unfamiliar technical guise.

A worked numerical example

To make Figure 17's equations concrete rather than purely symbolic, Figure 19 works through them on a small, explicitly synthetic wheat-protein dataset (n = 10), in the same illustrative spirit already established for Figure 11 earlier: no panel in Figure 19 is a measurement from a published study. Reference values and predictions are listed alongside their residuals (Panel A), plotted as a predicted-vs-reference scatter (Panel B), and reduced to the bias, RMSEP, SEP and R^2 figures defined in Figure 17 (Panel C). The worked arithmetic illustrates the review's recurring point in the most direct way available: bias (+0.19%) is small relative to RMSEP (0.28%), and RMSEP is close to SEP (0.22%), which is precisely the numerical signature of a model whose error is mostly random scatter rather than a hidden systematic offset , the diagnosis Panel B of Figure 17 argues a single, unaccompanied RMSEP value cannot support. A report that quotes only $R^2 = 0.977$ without the accompanying bias and SEP breakdown withholds exactly the information a reader would need to make that diagnosis.

(A) Illustrative worked example (synthetic wheat-protein data, n = 10)

	S1	S2	S3	S4	S5	S6	S7	S8	S9	S10
Reference y (%)	9.80	10.50	11.20	12.00	12.60	13.10	13.90	14.40	15.00	15.60
Predicted ŷ (%)	10.07	10.52	11.67	12.17	12.42	13.42	13.87	14.92	15.07	15.82
Residual (ŷ−y)	+0.27	+0.02	+0.47	+0.17	-0.18	+0.32	-0.03	+0.52	+0.07	+0.22

(B) Predicted vs reference

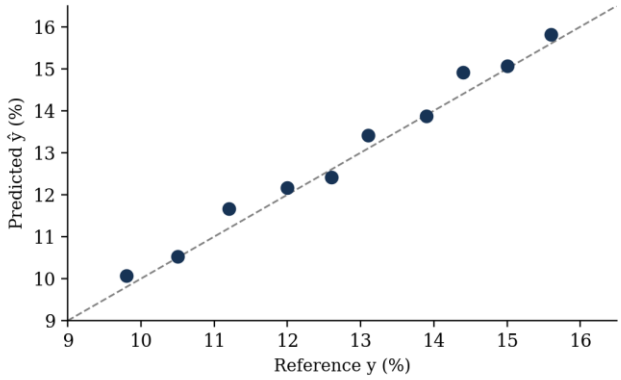

(C) Statistics computed from Figure 17's equations

$bias = +0.185$ %

$RMSEP = 0.280$ %

$SEP = 0.221$ %

$R^2 = 0.977$

A near-zero bias with RMSEP ≈ SEP indicates the error is mostly random scatter, not a systematic offset — exactly the distinction Figure 17B argues a single RMSEP hides.

Figure 19. Worked numerical example applying the validation-statistics equations of Figure 17 to a small, explicitly synthetic wheat-protein dataset (n = 10). (A) Reference, predicted and residual values; (B) predicted-vs-reference scatter; (C) resulting bias, RMSEP, SEP and R².

A minimum reporting checklist for NIR/HSI calibration studies

The review has repeatedly located the same gap in different technical guises: a claim is stated with a confidence its own evidentiary tier does not support, most often because a report omits the item that would let a reader tell the difference. Table 2 collects those omissions into a single, reusable checklist, cross-referenced to where this review discusses each item, intended for use by authors preparing a calibration report and by reviewers appraising one.

Table 2. Minimum reporting checklist for NIR/HSI calibration studies, consolidated from the evidentiary gaps identified throughout this review.

Checklist item	Minimum requirement	Where this is discussed
Validation set	State whether R²/RMSEP is cross-validated on the calibration pool (RMSECV) or computed on a genuinely independent, held-out test set (RMSEP); report both if available.	Fig. 17A, C
Bias and SEP	Report bias and SEP alongside RMSEP, not RMSEP alone, so a systematic offset can be distinguished from random scatter.	Fig. 17B; Fig. 19
Independence of test data	State explicitly whether the test set is from a different site, season, instrument unit or laboratory than the calibration set, or only a random split of the same batch.	Discussed above
Pre-processing pipeline	Report the specific pre-processing pipeline used (e.g., SNV, MSC, derivative order/window) and confirm it was re-optimised for this dataset rather than carried over from a previous study.	Fig. 11C
Wavelength/variable selection	Report the variable-selection method used, if any; accuracy figures are not comparable across studies unless the selection method is stated.	Literature table (Wang, 2021 entry)

Trait-level breakdown	Report accuracy per predicted trait/fraction rather than a single headline figure, where more than one property is predicted from the same model.	Fig. 16
Classification metrics beyond accuracy	For classification models, report a confusion matrix and Cohen's kappa (or equivalent chance-corrected statistic), not raw accuracy alone, particularly for imbalanced classes.	Fig. 5C, Fig. 17D
Radiometric/illumination calibration (UAV)	State the illumination-correction method used (e.g., single reference panel vs downwelling light sensor) and, if available, its own reported accuracy against reference panels.	Figs. 12–13
Evidentiary tier of cited support	When citing feasibility for a named product, method or platform, state whether the supporting citation is an independently reproduced result, a single-site demonstration, or a review-level synthesis.	Fig. 15; discussed above
Data and metadata availability	State whether the calibration spectra, reference values and instrument/processing metadata are deposited in a FAIR-compliant repository, and if not, why not.	Fig. 14

CONCLUSION

Taken together, this review gives a technically grounded, pedagogically organised account of NIR and hyperspectral sensing for crop- and food-matrix chemistry and structure, tracing the field from its historical and physical foundations through chemometric modelling to in-situ, on-machine and UAV-based deployment. The underlying sensing and chemometric techniques are technically sound and well established; the recurring critical finding of this review is one of calibration in the literal chemometric sense applied to confidence: named commercial products, worked examples, and preliminary or in-preparation findings are frequently presented across the wider literature with a level of assurance that does not always differentiate them from independently reproduced, peer-reviewed results. The cross-cutting statistical synthesis immediately above quantifies this finding: across the 34 independently selected sources underpinning this review, only a minority report genuinely independent, held-out validation, and the within-study accuracy ranges reported by the field's own best studies (Dowell et al., 2006; Caporaso et al., 2018; Schuster et al., 2023) show that a single headline accuracy figure routinely understates the range a reader should expect in practice. A reader intending to deploy a spectroscopic sensor operationally should treat introductory and vendor-facing material as a sound conceptual starting point only, and consult the independent, trial-level literature assembled in the reference list below, applying the evidentiary-tier and validation-statistics checklists of Figures 15 and 17, before committing to a specific instrument or calibration for a new crop, site, season or research programme.

REFERENCES

1. Aasen, H., Burkart, A., Bolten, A., & Bareth, G. (2015). Generating 3D hyperspectral information with lightweight UAV snapshot cameras for vegetation monitoring: From camera calibration to quality assurance. *ISPRS Journal of Photogrammetry and Remote Sensing*, *108*, 245-259. https://doi.org/10.1016/j.isprsjprs.2015.08.002
2. Aasen, H., Honkavaara, E., Lucieer, A., & Zarco-Tejada, P. J. (2018). Quantitative remote sensing at ultra-high resolution with UAV spectroscopy: a review of sensor technology, measurement procedures, and data correction workflows. *Remote Sensing*, *10*(7), 1091. https://doi.org/10.3390/rs10071091
3. Adão, T., Hruška, J., Pádua, L., Bessa, J., Peres, E., Morais, R., & Sousa, J. J. (2017). Hyperspectral imaging: a review on UAV-based sensors, data processing and applications for agriculture and forestry. *Remote Sensing*, *9*(11), 1110. https://doi.org/10.3390/rs9111110
4. Al-Tamimi, N., Langan, P., Bernád, V., Walsh, J., Mangina, E., & Negrão, S. (2022). Capturing crop adaptation to abiotic stress using image-based technologies. *Open Biology*, *12*(6), 210353. https://doi.org/10.1098/rsob.210353
5. Andries, J. P. M., & Vander Heyden, Y. (2024). Calibration transfer between NIR instruments using optimally predictive calibration subsets. *Analytical and Bioanalytical Chemistry*, *416*(24), 5351-5364. https://doi.org/10.1007/s00216-024-05468-6

6. Barnes, R. J., Dhanoa, M. S., & Lister, S. J. (1989). Standard normal variate transformation and de-trending of near-infrared diffuse reflectance spectra. *Applied Spectroscopy*, *43*(5), 772-777. https://doi.org/10.1366/0003702894202201
7. Behmann, J., Steinrücken, J., & Plümer, L. (2014). Detection of early plant stress responses in hyperspectral images. *ISPRS Journal of Photogrammetry and Remote Sensing*, *93*, 98-111. https://doi.org/10.1016/j.isprsjprs.2014.03.016
8. Ben-Gera, I., & Norris, K. H. (1968a). Determination of moisture content in soybeans by direct spectrophotometry. *Israel Journal of Agricultural Research*, *18*, 125-132.
9. Ben-Gera, I., & Norris, K. H. (1968b). Direct spectrophotometric determination of fat and moisture in meat products. *Journal of Food Science*, *33*, 64-67.
10. Beć, K. B., Grabska, J., & Huck, C. W. (2021). Principles and applications of miniaturized near-infrared (NIR) spectrometers. *Chemistry - A European Journal*, *27*(5), 1514-1532. https://doi.org/10.1002/chem.202002838
11. Bragagnolo, J., Amado, T. J. C., & Bortolotto, R. P. (2016). Use efficiency of variable rate of nitrogen prescribed by optical sensor in corn. *Revista Ceres*, *63*(1), 103-111. https://www.researchgate.net/publication/295264286_Use_efficiency_of_variable_rate_of_nitrogen_prescribed_by_optical_sensor_in_corn
12. Candiago, S., Remondino, F., De Giglio, M., Dubbini, M., & Gattelli, M. (2015). Evaluating multispectral images and vegetation indices for precision farming applications from UAV images. *Remote Sensing*, *7*(4), 4026-4047. https://doi.org/10.3390/rs70404026
13. Caporaso, N., Whitworth, M. B., & Fisk, I. D. (2018). Protein content prediction in single wheat kernels using hyperspectral imaging. *Food Chemistry*, *240*, 32-42.
14. Cherney, J. H., Digman, M. F., & Cherney, D. J. (2021). Handheld NIRS for forage evaluation. *Computers and Electronics in Agriculture*, *190*, 106469. https://www.sciencedirect.com/science/article/abs/pii/S0168169921004865
15. Dai, L., Luo, D., Zhang, J., Chen, Y., & Li, C. (2026). Near-infrared spectroscopy in food analysis: applications, chemometric strategies, and technological advances. *Foods*, *15*(10), 1814. https://doi.org/10.3390/foods15101814
16. Dowell, F. E., Maghirang, E. B., Xie, F., Lookhart, G. L., Pierce, R. O., Seabourn, B. W., Bean, S. R., Wilson, J. D., & Chung, O. K. (2006). Predicting wheat quality characteristics and functionality using near-infrared spectroscopy. *Cereal Chemistry*, *83*(5), 529-536. https://doi.org/10.1094/CC-83-0529
17. Fearn, T. (2001). Standardisation and calibration transfer for near infrared instruments: a review. *Journal of Near Infrared Spectroscopy*, *9*(4), 229-244. https://doi.org/10.1255/jnirs.309
18. Feiffer, A., Jasper, J., Leithold, P., & Feiffer, P. (2007). Effects of N-Sensor based variable rate N fertilization on combine harvest. https://www.researchgate.net/publication/290349564_Effects_of_N-Sensor_based_variable_rate_N_fertilization_on_combine_harvest
19. Feng, Y. Z., & Sun, D. W. (2012). Application of hyperspectral imaging in food safety inspection and control: a review. *Critical Reviews in Food Science and Nutrition*, *52*(11), 1039-1058.
20. Fodor, M., Matkovits, A., Benes, E. L., & Jókai, Z. (2024). The role of near-infrared spectroscopy in food quality assurance: a review of the past two decades. *Foods*, *13*(21), 3501. https://doi.org/10.3390/foods13213501
21. Geladi, P., & Kowalski, B. R. (1986). Partial least-squares regression: a tutorial. *Analytica Chimica Acta*, *185*, 1-17. https://doi.org/10.1016/0003-2670(86)80028-9
22. Gerhards, M., et al. (2019). Challenges and future perspectives of multi-/hyperspectral thermal infrared remote sensing for crop water-stress detection: a review. *Remote Sensing*, *11*(10), 1240.
23. Hagn, L., Mittermayer, M., Kern, A., Kimmelmann, S., Maidl, F.-X., & Hülsbergen, K.-J. (2025). Effects of sensor-based, site-specific nitrogen fertilizer application on crop yield, nitrogen balance, and nitrogen efficiency. *Sensors*, *25*(3), 795. https://doi.org/10.3390/s25030795
24. Huang, H., Liu, L., & Ngadi, M. O. (2014). Recent developments in hyperspectral imaging for assessment of food quality and safety. *Sensors*, *14*(4), 7248-7276. https://www.ncbi.nlm.nih.gov/pmc/articles/PMC4029639/
25. Kumar, K. (2021). Partial least square (PLS) analysis. *Resonance*, *26*, 747-759. https://doi.org/10.1007/s12045-021-1140-1

26. Maduro Dias, C., Nunes, H., & Borba, A. (2024). Near-infrared spectroscopy in animal nutrition: historical insights, technical principles, and practical applications. *Analytica*, *5*(4), 481-498. https://doi.org/10.3390/analytica5040033
27. Maertens, K., Reyns, P., & De Baerdemaeker, J. (2004). On-line measurement of grain quality with NIR technology. *Transactions of the ASAE*, *47*(4), 1135-1140. https://elibrary.asabe.org/abstract.asp?JID=3&AID=16545&CID=t2004&v=47&i=4&T=1
28. Maes, W. H., & Steppe, K. (2019). Perspectives for remote sensing with unmanned aerial vehicles in precision agriculture. *Trends in Plant Science*, *24*(2), 152-164.
29. Mahlein, A.-K. (2016). Plant disease detection by imaging sensors: parallels and specific demands for precision agriculture and plant phenotyping. *Plant Disease*, *100*(2), 241-251. https://doi.org/10.1094/PDIS-03-15-0340-FE
30. Mayfield, A. H., & Trengove, S. P. (2009). Grain yield and protein responses in wheat using the N-Sensor for variable rate N application. *Crop & Pasture Science*, *60*(9), 818-823. https://doi.org/10.1071/CP08344
31. McClure, W. F. (2003). 204 years of near infrared technology: 1800-2003. *Journal of Near Infrared Spectroscopy*, *11*(6), 487-518. https://doi.org/10.1255/jnirs.399
32. McQuilkin, G. L., & Engelke, G. L. (2020). Spectral imaging system for remote and noninvasive detection of target substances using spectral filter arrays and image capture arrays (US Patent No. 10,656,015). United States Patent and Trademark Office. https://image-ppubs.uspto.gov/dirsearch-public/print/downloadPdf/10656015
33. Medina-García, M., Amigo, J. M., Martínez-Domingo, M. A., Valero, E. M., & Jiménez-Carvelo, A. M. (2025). Strategies for analysing hyperspectral imaging data for food quality and safety issues: a critical review of the last five years. *Microchemical Journal*, *212*, 113487. https://www.sciencedirect.com/science/article/pii/S0026265X25013487
34. Mishra, P., Nikzad-Langerodi, R., Marini, F., Roger, J. M., Biancolillo, A., Rutledge, D. N., & Lohumi, S. (2021). Are standard sample measurements still needed to transfer multivariate calibration models between near-infrared spectrometers? The answer is not always. *TrAC Trends in Analytical Chemistry*, *143*, 116331. https://doi.org/10.1016/j.trac.2021.116331
35. Morales-Sillero, A., Fernández Pierna, J. A., Sinnaeve, G., Dardenne, P., & Baeten, V. (2018). Quantification of protein in wheat using near-infrared hyperspectral imaging: performance comparison with conventional NIR. *Journal of Near Infrared Spectroscopy*, *26*(3), 186-196.
36. Mulla, D. J. (2013). Twenty five years of remote sensing in precision agriculture: key advances and remaining knowledge gaps. *Biosystems Engineering*, *114*(4), 358-371. https://doi.org/10.1016/j.biosystemseng.2012.08.009
37. Nicolaï, B. M., Beullens, K., Bobelyn, E., Peirs, A., Saeys, W., Theron, K. I., & Lammertyn, J. (2007). Nondestructive measurement of fruit and vegetable quality by means of NIR spectroscopy: a review. *Postharvest Biology and Technology*, *46*(2), 99-118. https://doi.org/10.1016/j.postharvbio.2007.06.024
38. Rouse, J. W., Haas, R. H., Schell, J. A., & Deering, D. W. (1974). Monitoring vegetation systems in the Great Plains with ERTS. In *Third ERTS-1 Symposium* (NASA SP-351, pp. 309-317). NASA. https://ntrs.nasa.gov/citations/19740022614
39. Saha, D., & Manickavasagan, A. (2021). Machine learning techniques for analysis of hyperspectral images to determine quality of food products: a review. *Current Research in Food Science*, *4*, 28-38. https://www.sciencedirect.com/science/article/pii/S2665927121000034
40. SARE Grant Management System (2013). Final report for GNE12-039: Evaluation of NIR HarvestLab for accuracy and precision [Grant report]. Sustainable Agriculture Research & Education (SARE). https://projects.sare.org/project-reports/gne12-039/
41. Savitzky, A., & Golay, M. J. E. (1964). Smoothing and differentiation of data by simplified least squares procedures. *Analytical Chemistry*, *36*(8), 1627-1639. https://doi.org/10.1021/ac60214a047
42. Schuster, C., Huen, J., & Scherf, K. A. (2023). Prediction of wheat gluten composition via near-infrared spectroscopy. *Current Research in Food Science*, *6*, 100471. https://pmc.ncbi.nlm.nih.gov/articles/PMC10017355/
43. Selby, P., Abbeloos, R., Backlund, J. E., Basterrechea Salido, M., Bauchet, G., Benites-Alfaro, O. E., et al. (2019). BrAPI - an application programming interface for plant breeding applications. *Bioinformatics*, *35*(20), 4147-4155. https://doi.org/10.1093/bioinformatics/btz190

44. Shamshiri, R., et al. (2018). UAV-based NDVI mapping for crop-health assessment and disease detection. *Plant Disease*.
45. Singh, M., et al. (2015). Calibration and algorithm development for estimation of nitrogen in wheat crop using tractor-mounted N-sensor. *The Scientific World Journal*, *2015*, 163968.
46. Song, J., Liang, H., et al. (2025). Hyperspectral imaging: the intelligent eye to uncover the password of plant science. *Modern Agriculture*, *3*(2), e70026. https://doi.org/10.1002/moda.70026
47. Stall, S., Yarmey, L., Cutcher-Gershenfeld, J., Hanson, B., Lehnert, K., Nosek, B., Parsons, M., Robinson, E., & Wyborn, L. (2019). Make scientific data FAIR. *Nature*, *570*(7759), 27-29. https://doi.org/10.1038/d41586-019-01720-7
48. Swaminathan, V., Thomasson, J. A., Hardin, R. G., Rajan, N., & Raman, R. (2024). Radiometric calibration of UAV multispectral images under changing illumination conditions with a downwelling light sensor. *The Plant Phenome Journal*, *7*(1), e70005. https://doi.org/10.1002/ppj2.70005
49. Tremblay, N., Wang, Z., Ma, B. L., Bélec, C., & Vigneault, P. (2009). A comparison of crop data measured by two commercial sensors for variable-rate nitrogen application. *Precision Agriculture*, *10*(2), 145-161.
50. Tsouros, D. C., Bibi, S., & Sarigiannidis, P. G. (2019). A review on UAV-based applications for precision agriculture. *Information*, *10*(11), 349.
51. van Evert, F. K., Booij, R., Jukema, J. N., et al. (2012). Algorithms for sensor-based redistribution of nitrogen fertilizer in winter wheat. *Precision Agriculture*, *13*, 663-683.
52. Vines, T. H., Albert, A. Y. K., Andrew, R. L., Débarre, F., Bock, D. G., Franklin, M. T., Gilbert, K. J., Moore, J.-S., Renaut, S., & Rennison, D. J. (2014). The availability of research data declines rapidly with article age. *Current Biology*, *24*(1), 94-97. https://doi.org/10.1016/j.cub.2013.11.014
53. Wang, L., et al. (2021). Variable selection in near-infrared spectra: application to quantitative non-destructive determination of protein content in wheat. *Spectrochimica Acta Part A: Molecular and Biomolecular Spectroscopy*.
54. Westoby, M. J., Brasington, J., Glasser, N. F., Hambrey, M. J., & Reynolds, J. M. (2012). 'Structure-from-Motion' photogrammetry: a low-cost, effective tool for geoscience applications. *Geomorphology*, *179*, 300-314. https://doi.org/10.1016/j.geomorph.2012.08.021
55. Wilkinson, M. D., Dumontier, M., Aalbersberg, I. J., Appleton, G., Axton, M., et al. (2016). The FAIR guiding principles for scientific data management and stewardship. *Scientific Data*, *3*, 160018. https://doi.org/10.1038/sdata.2016.18
56. Workman, J. (2018). A review of calibration transfer practices and instrument differences in spectroscopy. *Applied Spectroscopy*, *72*(3), 340-365. https://doi.org/10.1177/0003702817736064
57. Yamada, W., Cherney, J., Cherney, D., Runge, T., & Digman, M. (2024). Handheld near-infrared spectroscopy for undried forage quality estimation. *Sensors*, *24*(16), 5136. https://pmc.ncbi.nlm.nih.gov/articles/PMC11359755/
58. Yang, G., et al. (2017). Unmanned aerial vehicle remote sensing for field-based crop phenotyping: current status and perspectives. *Frontiers in Plant Science*, *8*, 1111.
59. Yang, J., Li, J., Hu, J., Yang, W., Zhang, X., Xu, J., Zhang, Y., Luo, X., Ting, K. C., Lin, T., & Ying, Y. (2022). An interpretable deep learning approach for calibration transfer among multiple near-infrared instruments. *Computers and Electronics in Agriculture*, *192*, 106584.
60. Zeng, J., Guo, Y., Han, Y., et al. (2021). A review of the discriminant analysis methods for food quality based on near-infrared spectroscopy and pattern recognition. *Molecules*, *26*(3), 749. https://doi.org/10.3390/molecules26030749
61. Zhang, C., & Kovacs, J. M. (2012). The application of small unmanned aerial systems for precision agriculture: a review. *Precision Agriculture*, *13*, 693-712. https://doi.org/10.1007/s11119-012-9274-5